Published online 29 March 2022

Nucleic Acids Research, 2022, Vol. 50, No. 7 ***3817–3834***
https://doi.org/10.1093/nar/gkac189

Oxidative stress-CBP axis modulates MOB1 acetylation and activates the Hippo signaling pathway

Jiaqi Jin[1], Lei Zhang[1], Xueying Li[1], Weizhi Xu[1], Siyuan Yang[1], Jiagui Song[1], Wenhao Zhang[2], Jun Zhan[1], Jianyuan Luo[3] and Hongquan Zhang[1,*]

[1]Program for Cancer and Cell Biology, Department of Human Anatomy, Histology and Embryology, School of Basic Medical Sciences; Peking University International Cancer Institute; MOE Key Laboratory of Carcinogenesis and Translational Research and State Key Laboratory of Natural and Biomimetic Drugs, Peking University Health Science Center, Beijing 100191, China, [2]School of Life Sciences, MOE Key Laboratory of Bioinformatics, Tsinghua University, Beijing 100084, China and [3]Department of Medical Genetics, School of Basic Medical Sciences, Peking University Health Science Center, Beijing 100191, China

Received August 11, 2021; Revised February 19, 2022; Editorial Decision March 08, 2022; Accepted March 10, 2022

ABSTRACT

Reactive oxygen species (ROS) are constantly produced in cells, an excess of which causes oxidative stress. ROS has been linked to regulation of the Hippo pathway; however, the underlying detailed mechanisms remain unclear. Here, we report that MOB1, a substrate of MST1/2 and co-activator of LATS1/2 in the canonical Hippo pathway, interacts with and is acetylated at lysine 11 by acetyltransferase CBP and deacetylated by HDAC6. MOB1-K11 acetylation stabilizes itself by reducing its binding capacity with E3 ligase Praja2 and subsequent ubiquitination. MOB1-K11 acetylation increases its phosphorylation and activates LATS1. Importantly, upstream oxidative stress signals promote MOB1 acetylation by suppressing CBP degradation, independent of MST1/2 kinase activity and HDAC6 deacetylation effect, thereby linking oxidative stress to activation of the Hippo pathway. Functionally, the acetylation-deficient mutant MOB1-K11R promotes lung cancer cell proliferation, migration and invasion *in vitro* and accelerates tumor growth *in vivo*, compared to the wild-type MOB1. Clinically, acetylated MOB1 corresponds to better prediction of overall survival in patients with non-small cell lung cancer. Therefore, as demonstrated, an oxidative stress-CBP regulatory axis controls MOB1-K11 acetylation and activates LATS1, thereby activating the Hippo pathway and suppressing YAP/TAZ nuclear translocation and tumor progression.

INTRODUCTION

The classical Hippo signaling pathway mainly includes MST1/2 kinase, LATS1/2 kinase, their scaffold proteins SAV1, MOB1 and the primary downstream effectors YAP/TAZ. This pathway regulates cell proliferation, differentiation, survival and death, and thereby controls tissue growth, embryonic development and organ regeneration (1–5). In particular, MOB1 is an important co-activator in the Hippo pathway, belonging to the Mps One Binder (MOB) family. First discovered in yeast, the MOB family is highly conserved in evolution, which is crucial for cell survival, morphogenesis (6), spindle pole body duplication and mitotic exit network (7). In Drosophila melanogaster, the MOB family is divided into dMOB1, dMOB2, dMOB3 and dMOB4, which affects cell proliferation and death (8,9). Furthermore, four subfamilies have been identified in humans, including seven members, MOB1A, MOB1B (95% identical to MOB1A), MOB2, MOB3A, MOB3B, MOB3C and MOB4. In the classic Hippo signaling pathway, phosphorylated MST1/2 binds to MOB1 and releases MOB1 from an autoinhibitory state, promoting its interaction with LATS1/2 (10,11). Consequently, MST1/2 phosphorylates MOB1 at threonine 12 (T12) and threonine 35 (T35) (12), and phosphorylates LATS1/2 at the hydrophobic motif (HM) (13,14). Next, the MOB1-LATS1/2 complex separates from MST1/2, and MOB1 allosterically improves the autophosphorylation of LATS1/2 at the T-loop, leading to full activation of LATS1/2 (15). Furthermore, activated LATS1/2 promotes phosphorylation of YAP/TAZ, reduces YAP/TAZ nuclear translocation and inhibits the transcription of downstream target genes (16–18). Therefore, MOB1 is of great importance in the regulation of the Hippo signaling pathway.

*To whom correspondence should be addressed. Tel: +86 10 82802424; Fax: +86 10 82802424; Email: hongquan.zhang@bjmu.edu.cn
Present address: Hongquan Zhang, Ph.D., Program for Cancer and Cell Biology, Department of Human Anatomy, Histology and Embryology, School of Basic Medical Sciences, Peking University Health Science Center, #38 Xue Yuan Road, Beijing 100191, China.

An analysis, based on 9125 tumors in TCGA database, indicated that the Hippo pathway is one of the eight most frequently "altered" signaling pathways in human cancers, including lung cancer (19). Notably, the incidence and mortality of lung cancer in China are still very high among malignant tumors, and it was estimated to account for 27% of all cancer deaths in the United States (in 2015), 20% in the European Union (in 2016) and 18% all over the world (in 2020) (20,21). In addition, >80% of all lung cancer cases are non–small cell lung cancer, and the five-year survival rate of which is even <15% (20). It is reported that overexpression of MST1 in A549 cells promotes the phosphorylation of YAP, which inhibits cell proliferation and induces apoptosis (22). Furthermore, overexpression of LATS1 in H460 cells upregulates BAX and promotes apoptosis (23). In contrast, deletion of LATS1/2 genes in NSCLC cells could elevate the proliferation and migration of cancer cells. Therefore, the Hippo signaling pathway seems to play an inhibitory role in lung cancer. MOB1 is also considered to be a potential tumor suppressor, but detailed mechanism has not been determined and needs further investigations.

It is known that post-translational modifications (PTMs), such as phosphorylation, acetylation, methylation and ubiquitination have a notable effect on the activity of Hippo members. In addition to the phosphorylation at T12 and T35, as mentioned above, threonine 74 (T74) of MOB1 is another phosphorylation site by MST1/2, which is associated with the activation of NDR1 (12,24). Song *et al*. revealed the significant role of MOB1 in neurite growth and neurofunctional repair after spinal cord injury in mice, relying on the phosphorylation at serine 146 (S146) and promoting its degradation through the ubiquitin–proteasome pathway (25). Furthermore, ubiquitin ligase Praja2 facilitates the degradation of MOB1 and attenuates the Hippo pathway (26). A series of studies have also confirmed that MST1 (27), LATS1 (28) and YAP (29) can be acetylated, and all of them have a significant impact on the molecular functions and activation of the Hippo signaling pathway. However, the acetylation of MOB1 has not yet been explored, and thus, is the focus of this study.

Reactive oxygen species (ROS), including a series of molecular oxygen derivatives, such as hydrogen peroxide (H_2O_2), superoxide anions, peroxyhydrogen ions and hydroxyl radicals, are present in both normal and tumor cells. Normally, H_2O_2 produces H_2O via antioxidant molecules. Once oxidation and antioxidation are out of balance, excessive accumulation of H_2O_2 causes oxidative stress, subsequently promoting lipid oxidation and DNA damage (30,31). To combat this, organisms and cells emerge a series of responses. The Hippo pathway has been confirmed to be associated with oxidative stress or ROS, and MST1/2 is one of the most important Hippo members in ROS-mediated cell death and ROS resistance. For instance, MST1 is activated and enhances phosphorylation of FOXO3 under the stimulation of oxidative stress, mediating FOXO3 nuclear translocation and inducing neuronal cell death (32,33). MST1 is also related to ROS-dependent apoptosis in U2OS cells treated with cisplatin (34). In addition, oxidative stress can significantly downregulate the expression and activity of YAP in gastric cancer, breast cancer and bladder cancer cells (35–37). Together, these findings support that oxidative stress is an upstream regulator of the Hippo signaling pathway.

In addition to regulating phosphorylation, oxidative stress has also been shown to affect the level of acetylation, such as TyrRS (38,39), CHK2 (40), G6PD (41) and Hsp70 (42). Mechanistically, oxidative stress impacts the autoacetylation of CBP, which enhances its acetyltransferase activity (43). H_2O_2 treatment upregulates the PCAF levels (38). In addition, H_2O_2-induced oxidative stress can significantly increase the level and deacetylase activity of SIRT1 (40) and SIRT2 (44). Therefore, we hypothesized that oxidative stress is likely to affect various post-translational modifications.

In this study, we first determined that MOB1 can be acetylated at lysine 11, which is regulated by acetyltransferase CBP and deacetylase HDAC6. Oxidative stress, an upstream regulator of the Hippo pathway, markedly promotes MOB1 acetylation by stabilizing CBP. We linked MOB1 acetylation with activation of the Hippo signaling pathway and the progression of human lung adenocarcinoma.

MATERIALS AND METHODS

Cell lines

The human embryonic kidney cell line HEK293T was cultured in DMEM and the human lung adenocarcinoma cell line H1299 was cultured in RPMI1640, both of which were complemented by 10% heat inactivated fetal bovine serum (FBS), 100 U/ml penicillin and 100 mg/ml streptomycin, at the atmosphere of 37°C and 5% carbon dioxide.

Plasmids and siRNAs

The plasmids HA-CBP, HA-p300, FLAG-PCAF and HA-MOF were indicated in our previous publication (55). FLAG-HDAC1-7, Myc-HDAC8, FLAG-HDAC9 and LentiCRISPRv2 vectors were provided by Dr Jiadong Wang (Peking University Health Science Center, Beijing, China). HA-HDAC6 was provided by Dr Jun Zhou (College of Life Sciences, Nankai University, Tianjin, China). FLAG-MOB1 and HA-MOB1 were constructed by PCR-amplified human full-length MOB1 cDNA inserting into p3 × FLAG-CMV-10 vector (Sigma) and pCMV6-AC-3HA vector (OriGene). The FLAG-MOB1 and HA-MOB1 mutants were constructed by using Muta-direct™ Kit (Sbsgene, SDM-15). The sequences of full-length (1–216), the N-terminal (1–110) and C-terminal (111–216) domains of MOB1 were PCR-amplified and subcloned into pGEX-4T-1 vector (GE Healthcare), then GST-fusion MOB1 proteins were gotten. The sequences of DAC1 (1–503), DAC2 (448–840) and C-terminal (840–1215) of HDAC6 were PCR-amplified and inserted into pGEX-4T-1 vector (GE Healthcare), then GST-fusion HADC6 segments expression plasmids were obtained. The sequences of N-terminal domain (1–700), Bromo domain (701–1231), HAT domain (1232–1712) and C-terminal domain (1713–2441) of CBP were PCR-amplified and inserted into pCMV6-AC-3HA vector. And the sequence of full-length (1–216) of MOB1 was PCR-amplified and subcloned into pET–28a (+) vector (Novagen), and then His-fusion MOB1 proteins were purified.

The product codes or sequences of siRNAs against *STK3*, *STK4*, *CREBBP (CBP)* and *HDAC6* were shown below.

STK3: siB160407064054–1–5 of Guangzhou RiboBio Co., Ltd. (RiboBio);

STK4: siG081251114701–1–5 of Guangzhou RiboBio Co., Ltd. (RiboBio);

CREBBP (CBP): AACAGTGGGAACCTTGTTCCA;

HDAC6: CTGCAAGGGATGGATCTGA.

Antibodies and reagents

The antibodies utilized in this study were: MOB1 (Cell Signaling Technology, #13730, 1:1000), MOB1A (Santa Cruz, sc-393212, 1:1000 for western blot and 1:100 for immunoprecipitation), Acetylated-Lysine (Cell Signaling Technology, #9441, 1:1000), FLAG (Sigma, F1804, 1:5000), HA (Sigma, H3663, 1:2000), Myc (Abcam, ab32, 1:1000), CBP (Cell Signaling Technology, #7425, 1:1000), MST1 (Cell Signaling Technology, #14946, 1:1000), MST2 (Cell Signaling Technology, #3952, 1:1000), LATS1 (Cell Signaling Technology, #3477, 1:1000), YAP (Cell Signaling Technology, #14074, 1:1000), YAP/TAZ (Cell Signaling Technology, #8418, 1:1000), HDAC6 (Cell Signaling Technology, #7558, 1:1000), p-MOB1(T12) (Cell Signaling Technology, #8843, 1:1000), p-MOB1(T35) (Cell Signaling Technology, #8699, 1:1000), p-YAP(S127) (Cell Signaling Technology, #13008, 1:1000), p-YAP(S397) (Cell Signaling Technology, #13619, 1:1000), p-LATS1(T1079) (Cell Signaling Technology, #8654, 1:1000), p-TAZ(S89) (Cell Signaling Technology, #59971, 1:1000), Praja2 (Bethyl Laboratories, A302-991A, 1:1000), Actin (Proteintech, 60008-1-Ig, 1:3000), GAPDH (Abclonal, AC033, 1:10 000), and rabbit polyclonal antibody to acetylated MOB1 at K11 was produced using the peptide: SRSSK(Ac)TFKP (Jiaxuan Biotech, Beijing, China).

Transfection procedures were accomplished by using polyethylenimine (PEI) (Pol-yscience, 24765-1), Lipofectamine™ 2000 (Invitrogen, 11668019) and Lipofectamine™ RNAiMAX (Invitrogen, 13778150) followed protocols from the manufacturers. The class III sirtuin (SIRT) inhibitor nicotinamide (Sigma) and the histone deacetylase (HDAC) inhibitor Trichostatin A (TSA) (Sigma) were used respectively at a final concentration of 5 mM or 3 μM. Cycloheximide (Sigma), a eukaryote protein synthesis inhibitor, was at a final concentration of 100 mg/ml when added into the culture medium. In addition, the final concentration of MG132 (Selleck, S2619), a proteasome and calpain inhibitor, was 25 μM. The MST1/2 inhibitor, XMU-MP-1 (Selleck, S8334) was used at final concentration of 3 μM. Furthermore, the two reagents inducing oxidative stress, sodium arsenite (Sigma-Aldrich, S7400) and H_2O_2 (Bejing Chemical Works) and the antioxidant, N-Acetyl-L-cysteine (NAC) (Sigma-Aldrich, A7250-10G) were all added as indicated.

Co-immunoprecipitation and western blot analysis

Cells were washed by phosphate buffer saline (PBS) twice and lysed by protein lysis buffer (50 mM Tris-HCl, pH 7.4, 150 mM NaCl, 1% NP-40 or Triton X-100, 1 mM EDTA, 10 mM sodium butyrate and protease inhibitors) on ice for 0.5 h. Supernatant was collected after centrifugation and the concentration of protein was measured using Bicinchoninic acid (BCA) assay kit (Applygen, P1511-1). As for immunoprecipitation, protein solution was incubated with corresponding antibodies (3–10 μg) on end-over-end mixer overnight at 4°C, followed by supplementing 30–50 μl protein A/G agarose Beads (Santa Cruz, sc-2001/sc-2002). Subsequently, the reactive systems were incubated on end-over-end mixer for at least 4 h at 4°C, and the beads were washed for 3 times using lysis buffer (without protease inhibitors). Then protein solution or beads were boiled in SDS-PAGE loading buffer with β-mercaptoethanol for 10 min at 100°C and appropriate amount of protein was loaded into SDS-PAGE gels and transferred to PVDF membranes. The membranes were blocked in 5% skim milk for at least 1 h and then incubated with indicated antibodies for 4 h at room temperature or overnight at 4°C.

Real-time RT PCR

Trizol reagent (Invitrogen, 15596026) was utilized for cell total RNA isolating. cDNA was obtained by HiScript® Q RT SuperMix for qPCR (+gDNA wiper) (Vazyme Biotech Co.,Ltd, R12301) and amplified by real-time PCR in the reaction system of ChamQ Universal SYBR qPCR Master Mix (Vazyme Biotech Co., Ltd., Q711–02) using LightCycler® 96 (Roche) according to instrument specification. Three replicates were set for each sample and sequences of primers were shown below. Expression of each mRNA was standardized according to GAPDH.

H-ANKRD1-FOR: CAGACAAGAACAATCCAGATG;

H-ANKRD1-BAC: GCTCCAGCTTCCATTAACT;

H-CTGF-FOR: TTGCGAAGCTGACCTGGAA;

H-CTGF-BAC: TGCTGGTGCAGCCAGAAA;

H-CYR61-FOR: CACACCAAGGGGCTGGAATG;

H-CYR61-BAC: CCCGTTTTGGTAGATTCTGG;

H–CBP–FOR: CGGCTCTAGTATCAACCCAGG;

H–CBP–BAC: TTTTGTGCTTGCGGATTCAGT;

H–GAPDH–FOR: CAGCAAGAGCACAAGAGGAA;

H–GAPDH–BAC: CCCCTCTTCAAGGGGTCTAC.

GST pull-down assay

His-fusion proteins were obtained from *Escherichia coli* strains BL_{21} or Rosetta, incubated with HIS-Selected™ HF Nickel Affinity Gel (Sigma, H0537-25ML) and then eluted with imidazole in advance. GST–fusion proteins were purified from *E. coli* strains BL_{21} or Rosetta and incubated with 50 μl Glutathione–Sepharose 4B beads (GE Healthcare) for 2–4 h. His-fusion proteins were precleared using 25 μl GST protein and 50 μl Glutathione-Sepharose 4B beads for 2 h. Then, mix the prepared His-fusion proteins into the beads with GST-fusion proteins and incubated on end-over-end mixer overnight at 4°C. After washing with cold PBS for 3 times, the reaction mixture was boiled in SDS-PAGE loading buffer and subjected to western blot analysis with corresponding antibodies subsequently.

In vitro acetylation and deacetylation assay

In vitro acetylation assay was set up by mixing 2 μg HA-CBP protein eluted from HA-affinitive beads, 5 μg purified GST-fusion MOB1 protein and 20 μM acetyl-CoA into the acetylation reaction buffer (50 mM Tris-HCl pH 8.0, 0.1 mM EDTA,1 mM dithiothreitol and 10% glycerol) for 2 h at 30°C in water bath. In the case of *in vitro* deacetylation assay, the previous steps were similar to what has been described above. Then 2 μg of HA-HDAC6 protein eluted from HA-affinitive beads and deacetylation reaction buffer (25 mM Tris-HCl pH 8.0, 137 mM sodium chloride, 2.7 mM potassium chloride and 1 mM magnesium chloride) were added into the acetylation reaction systems at 30°C for 2 h. Subsequently, the samples were stopped by boiling in SDS-PAGE loading buffer and analyzed by western blot analysis with acetylated-lysine Ab or AcK11–MOB1 Ab.

Water-soluble tetrazolium salt 1 (WST1) assay

Cell proliferation ability was detected by WST1 assay. H1299 stably transfected cells were placed into 96-well plates at a density of 1.5×10^3 /well and the volume of cell culture medium was 100 μl/well. From the second day, added the reagent WST1 (Roche, 5015944001) every 24 h at the working dilution of 1:10 (10 μl/well) and incubated together for 0.5–4 h at 37°C and 5% CO_2. In addition, blank well (add 10 μl/well WST1 to 100 μl/well culture medium without cells) was set at the same time for every measure. Upon completion of incubation, the liquid mixture was subjected to quantitatively measurement using an ELISA microplate reader and the wavelength was 420–480 nm.

Plate colony formation assay

In plate colony formation assays, stably transfected H1299 cells were counted and suspended with culture medium containing 10% FBS. About 10^3 cells were seeded per well of 6-well dish and cultured in the incubator at 37°C, 5% CO_2 for 8–12 days. After fixed by 4% paraformaldehyde for 15 min, colonies were stained by crystal violet for 10 min, photographed and counted.

Transwell migration and invasion assays

The Transwell migration and invasion assays were accomplished by Transwell chambers (6.5 mm Insert, 24–well, 8 μm polycarbonate membrane) (Costar, 3422). In the invasion assay, 80 μl/well of Matrigel-culture medium mixture (the dilution ratio is 1:2–1:3) was added into each upper Transwell chamber at first and located in cell incubator until liquid solidifies. For cell migration assay, cells were counted and suspended in the culture medium with 0.5% FBS. About 100 μl of the suspension containing $2–5 \times 10^4$ cells were seeded into the upper Transwell chambers and 600 μl of the culture medium with 20–25% FBS or other specific chemotactic factors, such as collagen, was added into the bottom wells. Then, the culture systems were incubated at 37°C and 5% CO_2 for 6–8 h in the migration assay, or for 12–36 h in the invasion assay. After fixing by 4% paraformaldehyde for 15 min, cells which traversed through the Transwell membrane were stained by crystal violet for 10 min, photographed and counted.

Establishment of stable knockout cells using CRISPR/Cas 9 genome-editing system

Single guide RNA (sgRNA) target sequences of MOB1 were designed with the help of the Zhang Lab website-crispr design-Guide design resources and "Target Guide Sequence Cloning Protocol" of GeCKO. Then the oligos were cloned into LentiCRISPRv2 vector system after annealing. Human H1299 cells were transfected with sgRNA–cloned plasmids and treated with puromycin until all cells were dead in control group. Single cell colonies were dissociated with trypsin, planted into 96-well dishes respectively and cultured with completed medium (containing puromycin).

The three pairs of optimal sequences target MOB1 were shown below. And we used the first pair of oligos in the end.

#1 oligo1: CACCGCTCGGACCTGCAGACATGAC;
#1 oligo2: AAACGTCATGTCTGCAGGTCCGAGC;
#2 oligo1: CACCGTTCCATATAACATGTTGATC;
#2 oligo2: AAACGATCAACATGTTATATGGAAC;
#3 oligo1: CACCGAGCTGTCCAGTCATGTCTGC;
#3 oligo2: AAACGCAGACATGACTGGACAGCTC.

Ethics

The mice experiments (Permit Number: LA2017–008) and the studies on tissue samples of lung adenocarcinoma patients (Permit Number: ZRLW–5) were approved by the Ethics Committee of Peking University Health Science Center. All experiments on mice and human tumor samples were conducted in accordance with the Helsinki Declaration and its revised version.

In vivo xenograft tumorigenesis analysis

Male NU/NU nude mice (4–6 weeks old) were purchased from Beijing Vital River Laboratory Animal Technology Co., Ltd., maintained, and fed according to the stage (specific pathogen-free) and standard protocols. A total of 1×10^6 (per 100 μl) H1299 cells, stably overexpressing Vector, MOB1-WT or K11R mutant, were injected subcutaneously into the armpits of mice and each group consisted of six mice. After tumor formation, their sizes were measured and recorded every 2 days. The subcutaneous tumor masses were dissected at about 35 days, according to laboratory animal ethics, and the ultimate weights were measured simultaneously.

Patient tumor samples

To analyze the role of acetylation of MOB1-K11 in NSCLC, tumor samples were obtained from 85 lung adenocarcinoma patients, who had never been treated with neoadjuvant or adjuvant therapy before surgery, and had received surgery at Peking University Health Science Center from September 2004 to June 2009. The normal lung tissue samples, at least 3 cm away from tumor tissue, were obtained simultaneously from the same patients mentioned above. The patients included 47 males and 38 females, with an average age of 62 (range, 30–84). Survival was measured from surgery and ended with patient death. The median observation time for overall survival was 40 months (range, 1–92 month). Follow-up period was from November 2005 to

August 2014, during which time, 67 patients had died and the rest were still alive.

Immunohistochemical staining and assessment

The paraffin-embedded tissue sections were deparaffinized and rehydrated, following by incubation in 0.3% H_2O_2 for 30 min at room temperature to abrogate endogenous peroxidase activity. Antigen retrieval was accomplished using 10 mM sodium citrate buffer (pH 6.0) for 30 min. AcK11-MOB1 specific antibody was incubated at 4°C for 12 h and then PV6001 2-step plus Poly-HRP anti-Rabbit IgG Detection System (Zhongshanjinqiao, Beijing, China) was applied. Streptavidin-biotin-peroxidase method was used and the detection was accomplished by 3′3′-diaminobenzidine tetrahydrochloride (DAB) (D0430, Amresco, USA). Then hematoxylin was used to counterstain tissue sections and washed with flowing water for appropriate time. All immunostainings were assessed by pathologists and classified into strong staining group and low staining group.

Statistical analysis

The experiment results were analyzed with GraphPad Prism 6 software and displayed in the form of mean ± SD or SEM. Two-group datasets were compared by two-tailed Student's *t* test and three or more group datasets were compared by analyses of variance (ANOVA). All images or statistical results were based on at least three independent experiments. It is considered that * is for $P < 0.05$, ** is for $P < 0.01$, *** is for $P < 0.001$, and **** is for $P < 0.0001$.

RESULTS

MOB1 is acetylated by CBP at lysine 11

The phosphorylation and ubiquitination of MOB1, which significantly modulate the activation of Hippo pathway, have been reported previously (12,26,45). However, there are no reports on the acetylation of MOB1. We aimed to determine whether MOB1 can be acetylated and how acetylation regulates the function of MOB1. First, we performed immunoprecipitation with lysates of HEK293T cells using an acetylated-lysine (AcK) antibody, followed by detection using an MOB1 antibody. These results demonstrated that endogenous MOB1 can be acetylated (Figure 1A). Next, FLAG-MOB1 was immunoprecipitated by M2-Beads (anti-FLAG) and immunoblotted with an acetylated-lysine (AcK) antibody, indicating that exogenous MOB1 can also be acetylated (Supplementary Figure S1A). To identify the acetyltransferase of MOB1, we cotransfected MOB1 with a panel of acetyltransferases including CBP, p300, PCAF and MOF. The results showed that only CBP significantly promoted the acetylation of MOB1 (Figure 1B). Furthermore, we coexpressed MOB1 with CBP-WT or CBP-Y1503F (a catalytic activity-deficient mutant) and found that CBP-WT can acetylate MOB1, whereas CBP-Y1503F cannot (Supplementary Figure S1B). Subsequently, we overexpressed CBP with increasing amounts of the plasmid, and as expected, increased acetylation of MOB1 was observed (Supplementary Figure S1C). Thus, we concluded that MOB1 can be acetylated by CBP in living cells.

We then examined whether MOB1 interacted with CBP. HEK293T cells were lysed, and coimmunoprecipitation was performed with CBP antibody or IgG, followed by western blot analysis using an MOB1 antibody (Figure 1C). Then, exogenous (Supplementary Figure S1D) and endogenous (Supplementary Figure S1E) MOB1 were coimmunoprecipitated with HA-CBP in HEK293T cells. These findings suggest that both endogenous and exogenous MOB1 can interact with CBP in cells. To determine the region where MOB1 binds to CBP, we constructed four segments of CBP fused with GST and then expressed and purified the recombinant proteins from *E. coli*, including the N-terminus (1–700), Bromo domain (701–1231), HAT domain (1232–1712) and the C-terminus (1713–2441) (Supplementary Figure S1F). GST pull-down assays were performed using purified His-MOB1 protein and GST-CBP segments mentioned above. It was shown that MOB1 can bind directly to all four segments of CBP *in vitro*, although the interaction with the fourth segment was obviously weak (Supplementary Figure S1F, S1G). These results indicated that MOB1 indeed interacts with CBP.

Given that MOB1 is acetylated by CBP, we wanted to determine its acetylation sites. HEK293T cells were co-transfected with FLAG-MOB1 and HA-CBP, and MOB1 protein was enriched by immunoprecipitation using M2 beads, followed by SDS-PAGE electrophoresis. The gel was stained with Coomassie blue, and the band containing MOB1 was excised and analyzed by LC-MS/MS. Three potential MOB1 acetylation sites, lysine 11, lysine 17 and lysine 104 (K11, K17 and K104) were identified (Figure 1D). To determine which lysine is the major acetylation site, we constructed three K (lysine) to R (arginine) mutants, mimicking MOB1 acetylation-deficient conditions. FLAG-MOB1 (WT or three other mutants) and HA-CBP were coexpressed in cells and were immunoprecipitated with M2 beads. The results showed that the acetylation level of MOB1 decreased significantly in the K11R mutant group compared to MOB1-WT, K17R and K104R mutants, suggesting that the primary acetylation site of MOB1 is lysine 11 (Figure 1D, E).

Subsequently, to examine the endogenous lysine 11 acetylation, we prepared a rabbit polyclonal antibody specifically against acetylated-lysine 11 of MOB1 (AcK11-MOB1) using the synthetic peptide, SRSSK (AcK) TFKP. First, dot blot analysis was used to evaluate the specificity of this AcK11-MOB1 antibody, and the result demonstrated that AcK11-MOB1 antibody recognizes the K11 acetylated peptide rather than the unacetylated peptide (Figure 1F). Next, we transfected FLAG-MOB1-WT, K11R and K11Q mutants (mimics of MOB1 acetylation) with HA-CBP. Western blot analysis was performed using AcK11-MOB1 antibody and found that the antibody only recognizes MOB1-WT with CBP but not K11R or K11Q with CBP (Figure 1G). Moreover, we also transfected HA vector or HA-CBP plasmid in HEK293T cells, enriched endogenous MOB1 through immunoprecipitation with MOB1 Ab, and performed western blot using AcK11-MOB1 Ab. The results showed that endogenous MOB1 can be acetylated by CBP at K11, as expected, and acetylated MOB1 can be recog-

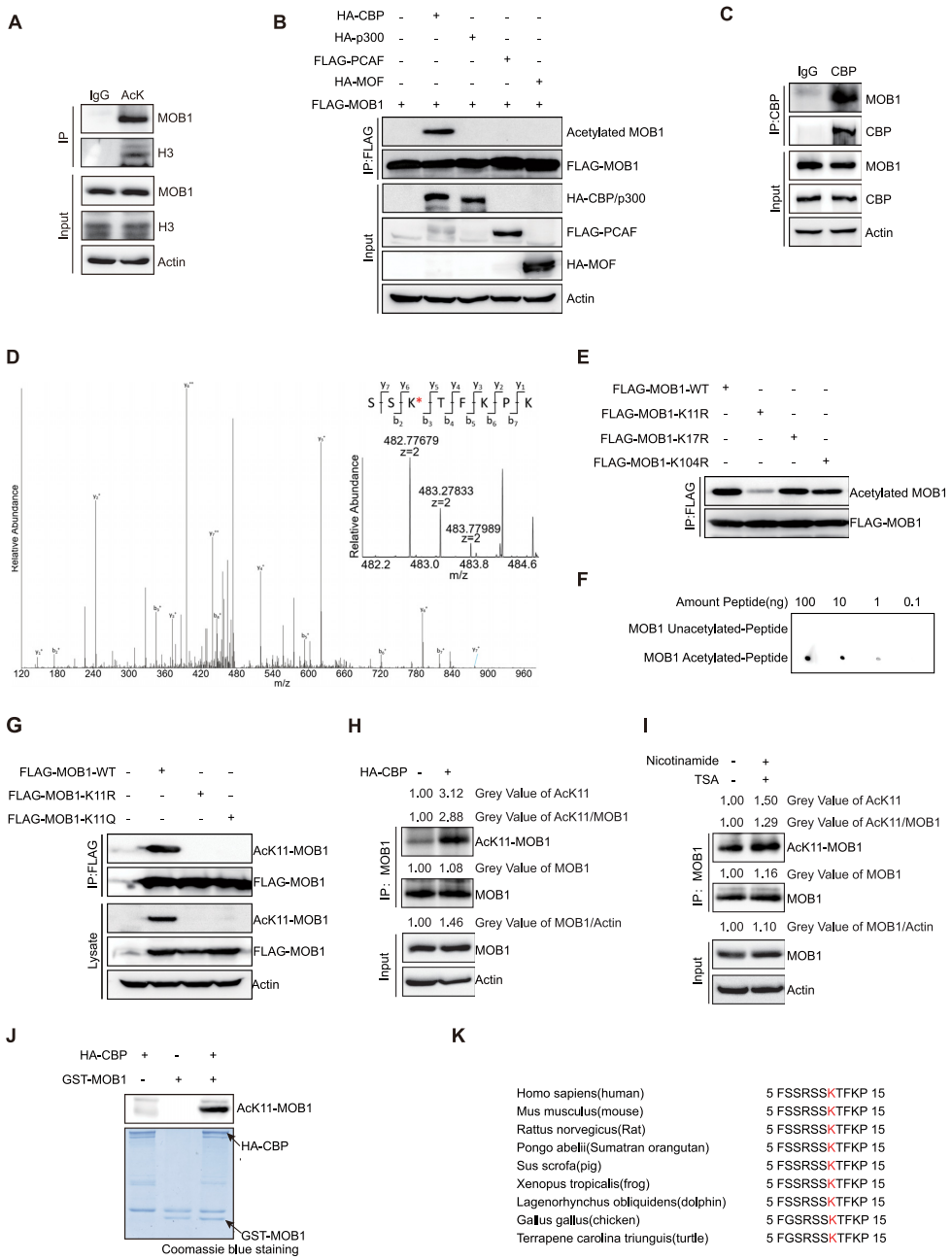

Figure 1. MOB1 is acetylated by CBP at lysine 11. (**A**) Lysates of wild-type HEK293T cells, treated with 5 mM nicotinamide and 3 μM TSA for 12 h before harvesting, were immunoprecipitated with antibody (Ab) to acetylated-lysine (AcK) or control IgG. Western blot analysis was applied with anti-MOB1 Ab, anti-H3 Ab and anti-Actin Ab in subsequent. (**B**) FLAG-MOB1 was coexpressed with diverse acetyltransferases, respectively, in HEK293T cells. Forty-eight hours after transfection, cells were lysed and performed immunoprecipitation with M2-Beads (anti-FLAG), followed by western blot analysis with the AcK Ab subsequently. (**C**) HEK293T cells were lysed and performed coimmunoprecipitation with antibody to CBP or IgG, and then detected by western blot analysis with MOB1 Ab. (**D**) The spectrum of the charged ion revealed that the lysine 11 of MOB1 (-SSK*TFKPK-) is acetylated by CBP. (**E**) HEK293T cells coexpressing HA-CBP and FLAG-MOB1 (wild-type or mutation at different sites individually) were performed immunoprecipitation with M2-Beads (anti-FLAG) and then immunoblotted with AcK Ab and FLAG Ab. (**F**) The dot blot assay was performed to confirm the specificity of the antibody to AcK11-MOB1 (AcK11-MOB1 Ab). MOB1 unacetylated-peptide and acetylated-peptide with different concentrations were dotted on Nitrocellulose membrane and were detected by AcK11-MOB1 Ab. (**G**) HEK293T cells were transfected with FLAG-MOB1-WT, K11R or K11Q plasmids, respectively. A part of cell lysates was performed immunoprecipitation with M2-Beads (anti-FLAG) and then immunoblotted with the AcK11-MOB1 Ab. Another part of the lysates was directly detected by SDS-PAGE and immunoblotted with the AcK11-MOB1 Ab. (**H**) HEK293T cells were transfected with HA-CBP or HA-tagged vector, and lysed 48 h later. Cell lysates were performed immunoprecipitation with MOB1 Ab, followed by western blot analysis using AcK11-MOB1 Ab, MOB1 Ab or Actin Ab. The gray value of the bands was quantified using ImageJ and labeled above the bands. (**I**) Lysates of HEK293T cells, which were treated with 5 mM nicotinamide and 3 μM TSA for 12 h before harvesting, were immunoprecipitated with MOB1 Ab and immunoblotted with the AcK11-MOB1 Ab, MOB1 Ab or Actin Ab subsequently. The gray value of the bands was quantified using ImageJ and labeled above the bands. (**J**) *In vitro* acetylation assays were accomplished with purified GST, GST-fusion protein of MOB1 and HA-CBP (eluted from HA-affinitive beads in advance). Then SDS-PAGE and immunoblotting with the AcK11-MOB1 Ab were performed. The purified GST-MOB1 and eluted HA-CBP were exhibited by Coomassie blue staining. (**K**) The amino acids adjacent to human MOB1-K11 are of high conservation in diverse species.

nized by this antibody (Figure 1H). In addition, we ectopically expressed FLAG-MOB1 in HEK293T cells (Supplementary Figure S1H) or used the wild-type HEK293T cells (Supplementary Figure S1I), in which endogenous CBP was knocked down with small interfering RNA (siRNA). The results showed that in both cases, knockdown of CBP led to the decrease of MOB1 acetylation at lysine 11, confirming again that CBP acetylates MOB1 at lysine 11. Furthermore, it was known that deacetylases are classified into two categories: histone deacetylase (HDAC) family and sirtuin (SIRT) family (46,47), the inhibitors of which are trichostatin A (TSA) and nicotinamide, respectively. HEK293T cells were treated with TSA and nicotinamide simultaneously, and immunoprecipitation was performed using the MOB1 Ab, followed by western blot analysis with AcK11-MOB1 Ab. Here, we observed an upregulation of endogenous MOB1 acetylation (Figure 1I). Then, we performed *in vitro* acetylation assays using purified GST-fusion protein of MOB1 and HA-CBP. GST pull-down experiments demonstrated that AcK11-MOB1 antibody can recognize MOB1 acetylation not only in living cells but also for the purified proteins *in vitro* (Figure 1J). In addition, we performed sequence alignment for MOB1 homology in nine different species as indicated, displaying that the amino acids adjacent to human MOB1-K11 are highly conserved in comparing with other species (Figure 1K). Altogether, these data demonstrated that lysine 11 is the acetylation site of MOB1 by CBP, which is highly conserved during evolution.

HDAC6 interacts with and deacetylates MOB1

Acetylation and deacetylation are dynamic processes; thus, we intended to determine the deacetylases of MOB1. First, we transfected FLAG-MOB1 in HEK293T cells and treated them with nicotinamide or TSA for 12 h. The results showed that only TSA was able to increase the acetylation of MOB1 at lysine 11, suggesting that its deacetylase belongs to the HDAC family (Figure 2A). Then, we coexpressed FLAG-MOB1 with different HDAC expression plasmids separately. The results demonstrated that HDAC1, HDAC6 and HDAC8 decreased the level of acetylation of MOB1 at lysine 11, among which HDAC6 showed the strongest effect (Figure 2B,C). Next, the acetylation of MOB1 at lysine 11 increased as expected after HDAC6 knockdown by siRNA (Figure 2D). It is also shown that MOB1 deacetylation by HDAC6 can be rescued by TSA treatment in cells (Figure 2E). Furthermore, MOB1 deacetylation by HDAC6 *in vitro* was examined using purified FLAG-HDAC6, HA-CBP and GST-MOB1 (Supplementary Figure S2A). Thus, we demonstrated that HDAC6 deacetylates MOB1.

To examine the interaction between MOB1 and HDAC6, we coexpressed FLAG-MOB1 and HA-HDAC6 in HEK293T cells and found that exogenous HDAC6 could be coimmunoprecipitated with FLAG-MOB1 (Figure 2F). Conversely, exogenous MOB1 can be coimmunoprecipitated with FLAG-HDAC6 (Figure 2G). In addition, HEK293T cells were transfected with FLAG-HDAC6 and subjected to a co-immunoprecipitation assay, and the results showed that endogenous MOB1 interacts with FLAG-HDAC6 (Figure 2H). Furthermore, we constructed a series of GST-fusion HDAC6 plasmids, DAC1 (1–503), DAC2 (448–840) and the C-terminal domain (840–1215), and performed GST pull-down assays with purified His-MOB1 protein. The results showed that MOB1 can bind to all three segments of HDAC6, and the DAC1 domain showed a stronger interaction with MOB1 than the DAC2 domain (Supplementary Figure S2B, S2C). In summary, these experiments demonstrated that HDAC6 deacetylates and interacts with MOB1 both *in vivo* and *in vitro*.

Acetylation of MOB1 increases its stability

Acetylation is known to impact protein–protein interactions (48,49), subcellular localization (50), enzymatic activity (51–53), gene transcription (54), cellular metabolism (41) and protein stability (46), as seen in the regulation of the stability of EZH2 (55) and SRSF5 (56). We wanted to determine whether acetylation affects the stability of MOB1. First, we transfected HA-CBP (Supplementary Figure S3A) or knocked down CBP using siRNA (Supplementary Figure S3B), and discovered that endogenous MOB1 increases or decreases prominently in both H1299 and HEK293T cells. Analogously, when treated with TSA, the protein level of MOB1 raised because of the up-regulation of MOB1 acetylation (Supplementary Figure S3C). Therefore, we assumed that acetylation may influence the protein stability of MOB1. To confirm that, we cotransfected HA-CBP with FLAG-MOB1-WT or K11R mutant in H1299 (Figure 3A) and HEK293T cells (Figure 3C), and then treated the cells with cycloheximide (CHX), an inhibitor of protein synthesis, for the indicated hours. The results showed that half-life of MOB1-K11R mutant was markedly shorter than that of MOB1-WT (Figure 3A–D). In addition, we also coexpressed FLAG-MOB1 with HA-CBP or HA-CBP-Y1503F mutant in both H1299 (Supplementary Figure S3D) and HEK293T cells (Supplementary Figure S3F), and then repeated the experiments. Results showed that the half-life of FLAG-MOB1 with HA-CBP-Y1503F was significantly shorter than that of FLAG-MOB1 with wild-type CBP (Supplementary Figure S3D–G), indicating again that hyperacetylation stabilizes MOB1.

To explore the underlying mechanism, we cotransfected FLAG-MOB1 and HA-ubiquitin with HA-CBP-WT or Y1503F mutant in both H1299 (Figure 3E) and HEK293T cells (Figure 3F). The results showed that ubiquitination of exogenous MOB1 decreased under hyperacetylation (Figure 3E,F). Moreover, the ubiquitination level of MOB1 decreased when HDAC6 was inhibited by TSA (Figure 3G,H) or depleted by siRNA (Supplementary Figure S3H, S3I). Together, these results demonstrated that the acetylation of MOB1 can reduce its polyubiquitination level. Furthermore, we expressed FLAG-MOB1-WT or K11R mutant with HA-ubiquitin in H1299 (Figure 3I) and HEK293T cells (Figure 3J), and the K11R mutant exhibited a more apparent ubiquitination, as expected (Figure 3I, J). Praja2, an E3 ligase, is reported to mediate the ubiquitination and degradation of MOB1 (26). Hence, we performed coimmunoprecipitation in cells transfected with FLAG-MOB1-WT or K11R mutant, and the results showed that MOB1-K11R mutant had a stronger interaction with Praja2, which degraded much faster than MOB1-WT (Supplementary

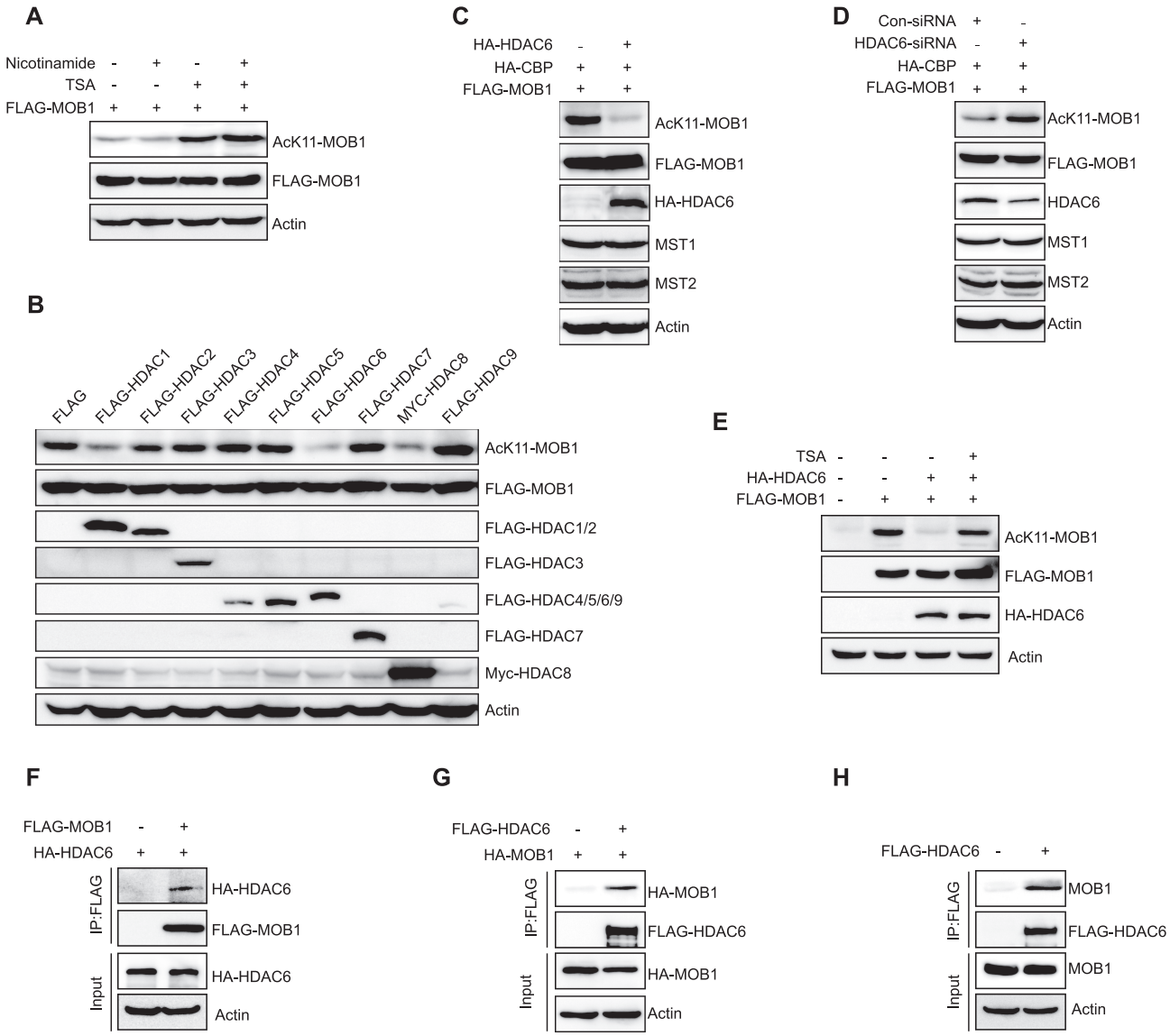

Figure 2. HDAC6 interacts with and deacetylates MOB1. (**A**) HEK293T cells expressing FLAG–MOB1 were treated with 5 mM nicotinamide or 3 μM TSA for 12 h before harvesting, and the lysates were detected by SDS-PAGE and immunoblotting with the AcK11-MOB1 Ab. (**B**) FLAG-MOB1 was co-transfected with HA–CBP and diverse histone deacetylase (HDACs) plasmids in HEK293T cells, and cell lysates were detected by SDS-PAGE and immunoblotting with indicated antibodies. (**C**) HEK293T cells were cotransfected with FLAG-MOB1, HA-CBP and HA-HDAC6, the lysates were analyzed by western blot analysis using indicated antibodies. (**D**) HEK293T cells, cotransfected with FLAG-MOB1 and HA-CBP, together with or without siRNA against *HDAC6*, were lysed. Lysates were detected by SDS-PAGE and immunoblotting with indicated antibodies. (**E**) HEK293T cells cotransfected with FLAG-MOB1 and HA-HDAC6 were treated with or without 3 μM TSA for 12 h before harvesting, followed by immunoblotting. (**F**–**H**) FLAG-MOB1 together with HA-HDAC6 (F), HA-MOB1 with FLAG-HDAC6 (G) or FLAG-HDAC6 separately (H) were transfected in HEK293T cells. Lysates were coimmunoprecipitated with M2–Beads (anti-FLAG) and then immunoblotted with indicated antibodies.

Figure S3J, S3K). Therefore, acetylation stabilizes MOB1 by weakening the interaction between MOB1 and its E3 ligase, Praja2.

MOB1 acetylation regulates Hippo signaling pathway

MOB1 is an important component of the Hippo signaling pathway and is required for full activation of the Hippo core kinase LATS1 (3,12,57,58). To examine whether acetylation plays a role in the regulation of MOB1 phosphorylation, FLAG-MOB1 and HA-CBP were cotransfected in HEK293T cells, followed by immunoprecipitation and western blot analysis. The results showed that MOB1 acetylation increased its phosphorylation at both T12 and T35 sites (Supplementary Figure S4A), and T12 seemed to show a much stronger phosphorylation than T35. To avoid endogenous MOB1 interference, we constructed MOB1 stable knockout (KO) H1299 cells (Supplementary Figure S4B). Then, we expressed FLAG-MOB1-WT and K11R mutant separately in H1299 KO cells, and immunoprecipitated exogenous MOB1. The results showed that K11R mutant remarkably decreased MOB1 phosphorylation at T12 (Figure 4A), and the same results were observed in HEK293T cells (Figure 4B). In addition, similar changes were also

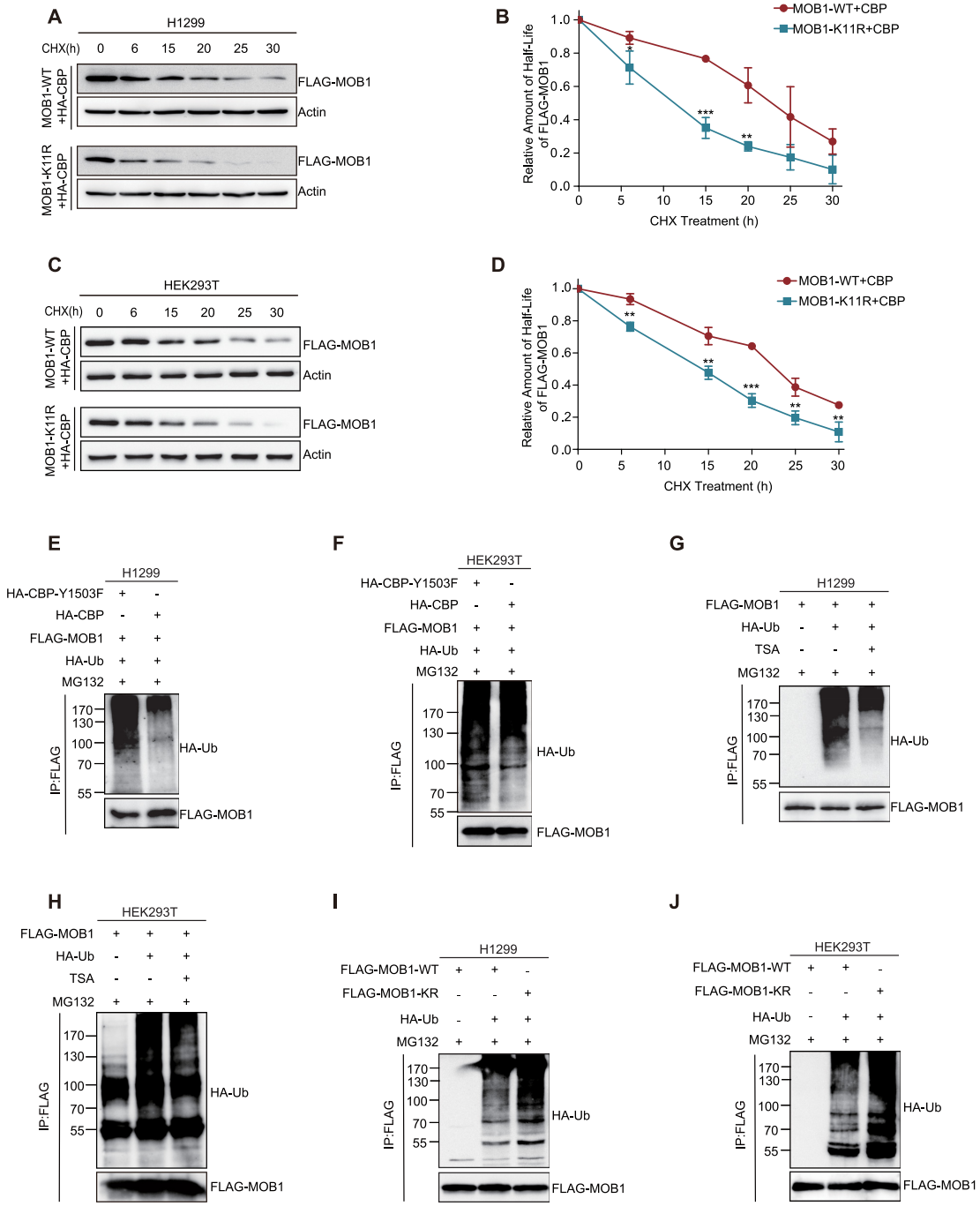

Figure 3. Acetylation of MOB1 increases its stability. (**A** and **B**) FLAG-MOB1-WT (upper part) or FLAG-MOB1-K11R mutant (bottom part) were cotransfected with HA-CBP in H1299 cells, then treated with 100 mg/ml cycloheximide (CHX) for indicated hours before harvesting. Cell lysates were performed western blot analysis with FLAG Ab and Actin Ab to examine the half-life (A). The curves were completed based on the gray value quantification of the bands of FLAG-MOB1 in (A) by software ImageJ and GraphPad Prism 6. Error bars were representing means ± SD. According to two-tailed Student's *t*-test,* is for $P < 0.05$, ** is for $P < 0.01$ and *** is for $P < 0.001$. Images and statistical results were based on three independent experiments (B). (**C** and **D**) FLAG-MOB1-WT (upper part) or FLAG-MOB1-K11R mutant (bottom part) were cotransfected with HA-CBP in HEK293T cells, then treated with 100 mg/ml cycloheximide (CHX) for indicated hours before harvesting. Cell lysates were subjected to western blot analysis with FLAG Ab and Actin Ab to determine the half-life (C). The curves were completed based on the gray value of the FLAG-MOB1 bands in (C) by ImageJ and GraphPad Prism 6. Error bars represent means ± SD. According to two-tailed Student's *t*-test, ** is for $P < 0.01$ and *** is for $P < 0.001$. Images and statistical results were based on three independent experiments (D). (**E** and **F**) H1299 (E) or HEK293T cells (F) transiently co-expressing FLAG-MOB1, HA-ubiquitin and HA-CBP (WT or Y1503F mutant) were treated with 25 μM MG132 for 12 h before harvesting. Lysates were performed immunoprecipitation with M2-Beads (anti-FLAG) and then immunoblotted with HA Ab and FLAG Ab. (**G** and **H**) H1299 (G) or HEK293T cells (H) were cotransfected FLAG-MOB1 and HA-ubiquitin, and then treated with 25 μM MG132, together with or without 3 μM TSA for 12 h before harvesting. Lysates were performed immunoprecipitation with M2-Beads (anti-FLAG) and then immunoblotted with HA Ab and FLAG Ab. (**I** and **J**) H1299 (I) or HEK293T cells (J) were transiently cotransfected with FLAG-MOB1 (WT or K11R mutant) and HA-Ubiquitin, and then treated with 25 μM MG132 for 12 h before harvesting. Lysates were performed immunoprecipitation with M2-Beads (anti-FLAG) and immunoblotted with HA Ab and FLAG Ab.

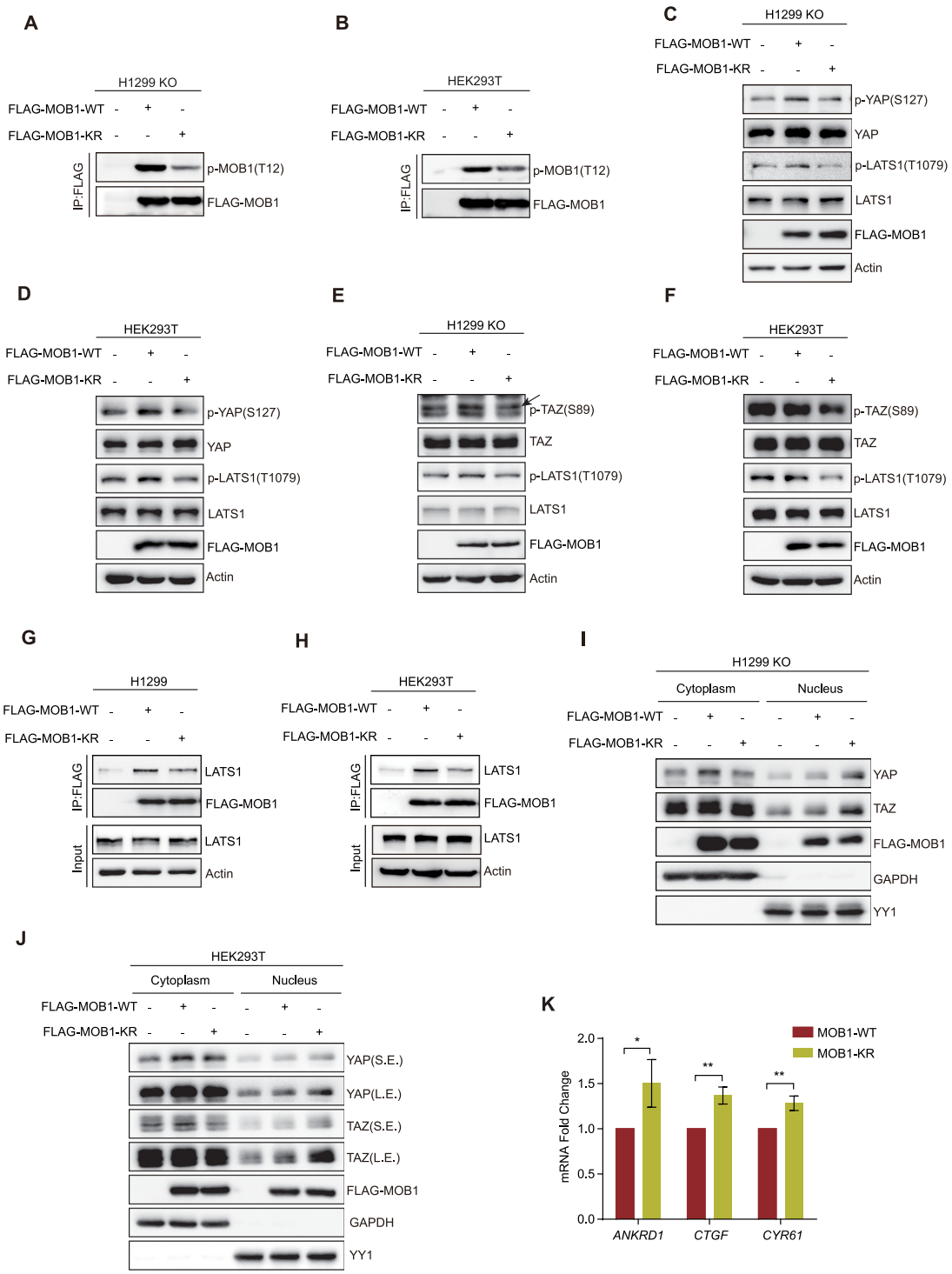

Figure 4. Acetylation of MOB1 regulates Hippo signaling pathway. (**A** and **B**) FLAG-MOB1 plasmids (WT or K11R mutant) were expressed respectively in H1299 KO cells (A) or HEK293T cells (B). Cell lysates were immunoprecipitated with M2-beads (anti-FLAG) and followed by immunoblotting with the p-MOB1 (T12) Ab and FLAG Ab. (**C–F**) H1299 KO cells (C,E) or HEK293T cells (D,F) were transfected with FLAG-MOB1 (WT or K11R mutant), and the lysates were subjected to immunoblotting with p-YAP (S127) Ab (C,D), p-TAZ (S89) Ab (E,F), p-LATS1 (T1079) Ab, FLAG Ab and Actin Ab (C–F). (**G** and **H**) H1299 (G) or HEK293T cells (H) transfected with FLAG-MOB1 (WT or K11R mutant) were coimmunoprecipitated with M2-Beads (anti-FLAG) and then immunoblotted with the indicated antibodies. (**I** and **J**) H1299 KO cells (I) or HEK293T cells (J) were transfected with FLAG-MOB1 (WT or K11R mutant), and then nuclear and cytoplasmic proteins were extracted. Nuclear proteins and cytoplasmic proteins were subjected to western blot analysis respectively with YAP, TAZ, FLAG, GAPDH (reference gene for cytoplasm) and YY1 (reference gene for nucleus) antibodies. S.E. means short exposure. L.E. means long exposure. (**K**) FLAG-MOB1-WT or K11R mutant was expressed respectively in H1299 KO cells, and endogenous *ANKRD1*, *CTGF* and *CYR61* mRNA expression levels were detected by qPCR. Statistical analyses were performed by GraphPad Prism 6, and error bars represent means ± SD. According to two-tailed Student's *t*-test, * is for $P < 0.05$ and ** is for $P < 0.01$. Images and statistical results were based on three independent experiments.

observed at T35, but the effect was far less pronounced than that at T12 (Supplementary Figure S4C, S4D). Importantly, we discovered that K11R mutant decreased LATS1 phosphorylation at T1079, YAP phosphorylation at S127, and TAZ phosphorylation at S89 in H1299 KO cells and HEK293T cells (Figure 4C–F). Among them, LATS1 phosphorylation at T1079 marks its activation, and YAP phosphorylation at S127 or TAZ phosphorylation at S89 are closely related to their binding to 14–3-3 and cytoplasmic retention. Moreover, to examine whether MOB1 acetylation affects its interaction with LATS1, we performed a coimmunoprecipitation assay. The results confirmed that the interaction between LATS1 and MOB1-K11R mutant was much weaker than that between LATS1 and wild-type MOB1 (Figure 4G,H), suggesting that MOB1 acetylation is required for the LATS1-MOB1 interaction. To determine the effect of MOB1 acetylation on YAP/TAZ localization, we prepared nuclear and cytoplasmic protein extractions in H1299 KO cells or HEK293T cells, transfected with FLAG-MOB1-WT and K11R mutant separately. The results showed that MOB1-WT retained more YAP/TAZ in the cytoplasm, whereas MOB1-K11R promoted more YAP/TAZ in the cell nucleus (Figure 4I,J). Additionally, we performed qPCR assays in H1299 KO cells to understand the effect of MOB1 acetylation on the transcription levels of YAP/TAZ target genes in cancer cells. The results showed that MOB1 acetylation-deficient mutant K11R upregulated expression of the Hippo target genes *ANKRD1*, *CYR61* and *CTGF* (Figure 4K), which was in agreement with the finding that K11R promotes YAP/TAZ nuclear translocation (Figure 4I,J). In conclusion, these data indicated that acetylation of MOB1 promotes its phosphorylation and the binding capacity with LATS1 and then inhibits YAP/TAZ nuclear translocation.

To investigate whether MOB1 acetylation is modulated by upstream signaling in the Hippo pathway network, we first determined whether MOB1 phosphorylation by MST1/2 has an effect on its acetylation. We cotransfected FLAG-MOB1 with HA-MST1 or MST2, and found that expression of MST1/2 led to an increase in MOB1 phosphorylation at both T12 and T35, with concomitant enhancement of MOB1 acetylation (Supplementary Figure S4E). Furthermore, cells expressing FLAG-MOB1 were treated with different concentrations of the MST1/2 inhibitor XMU-MP-1, followed by western blot analysis. The results indicated that inhibition of the catalytic activity of MST1/2 led to a decrease in MOB1 phosphorylation and suppression of MOB1 acetylation (Supplementary Figure S4F), with concomitant inactivation of LATS1 and YAP. Therefore, MOB1 phosphorylation by MST1/2 affects its acetylation and subsequent activation of LATS1 and YAP. To identify which phosphorylation site (T12 or T35) is responsible for MOB1 acetylation, we generated T (threonine) to A (alanine), or T (threonine) to D (aspartic acid) mutant plasmids as indicated in the Supplementary Figure S4G, which mimic phosphorylation-deficient and hyperphosphorylation conditions, respectively. By detecting AcK11-MOB1, we found that only the MOB1 T35A mutant drastically reduced the acetylation of MOB1 (Supplementary Figure S4G). Notably, the addition of the upstream kinase MST2 cannot reverse this phenomenon (Supplementary Figure S4G). These findings suggested that T35 plays a key role in the acetylation of MOB1. Hence, we demonstrated that there is crosstalk between MOB1 acetylation and phosphorylation, and these two PTMs synergistically regulate the Hippo signaling pathway.

Oxidative stress-CBP axis regulates MOB1 acetylation

It is known that ROS are higher in tumors than in normal tissues from the same source. The metabolism of cancer cells is significantly enhanced and cell injury prompts cytokine infiltration, which aggravates oxidative stress during the development of lung cancer (30,31). Moreover, it has been reported that oxidative stress activates MST1/2 in several cell lines (32–34,59). To examine whether oxidative stress regulates MOB1 acetylation and consequently modulates the Hippo pathway, we transiently transfected FLAG-MOB1 in HEK293T cells and treated cells with 1 mM oxidative stress inducers, sodium arsenite or hydrogen peroxide (H_2O_2) (Figure 5A,B) for various times as indicated. The results showed that acetylation of exogenous MOB1 increased with longer exposure to sodium arsenite or H_2O_2 treatment (Figure 5A,B). Similarly, cells expressing FLAG-MOB1 were treated with various concentrations of sodium arsenite or H_2O_2 for 1 h, and the acetylation level increased with increasing doses of sodium arsenite or H_2O_2 (Figure 5C,D). More importantly, endogenous MOB1 acetylation also showed a significant upregulation under the induction of sodium arsenite or H_2O_2 (Figure 5E,F). Therefore, MOB1 is also an effector of oxidative stress, responding quickly and effectively.

It has been reported that the autoacetylation of CBP at K1535 is enhanced, and its catalytic activity increases under the stimulation of oxidative stress (43), which may explain the phenomenon we observed here. Moreover, we also found that the protein level of endogenous CBP was significantly increased with longer time or larger doses of sodium arsenite or H_2O_2 treatment (Figure 5A–D). To examine whether oxidative stress is involved in regulating CBP levels, we applied N-acetyl-L-cysteine (NAC), an antioxidant that protects cells against oxidative stress. As shown in Supplementary Figure S5A, the increase in CBP protein, promoted by the oxidative stress inducer H_2O_2, can be blocked by the addition of NAC, while MOB1 acetylation also declined. Furthermore, the level of HDAC6 remained unchanged (Figure 5A–D), suggesting that oxidative stress can regulate MOB1 acetylation by increasing the level of CBP, but not decreasing the level of HDAC6.

To uncover the mechanism underlying the elevation of CBP induced by oxidative stress, we first measured the mRNA expression of *CBP*. Surprisingly, we found that *CBP* mRNA was reduced after stimulation for 1 h by the two oxidative inducers (Figure 5G), which is obviously not in agreement with the above notion that sodium arsenite or H_2O_2 treatment stabilize CBP. How to interpret this phenomenon? We hypothesized that treatment of oxidative stress might slow down the degradation of CBP while its gene expression is also downregulated, and resulting in the accumulation of CBP protein. To test this hypothesis, we first examined the possible pathways that mediate CBP degradation and found that CBP was raised distinctly after

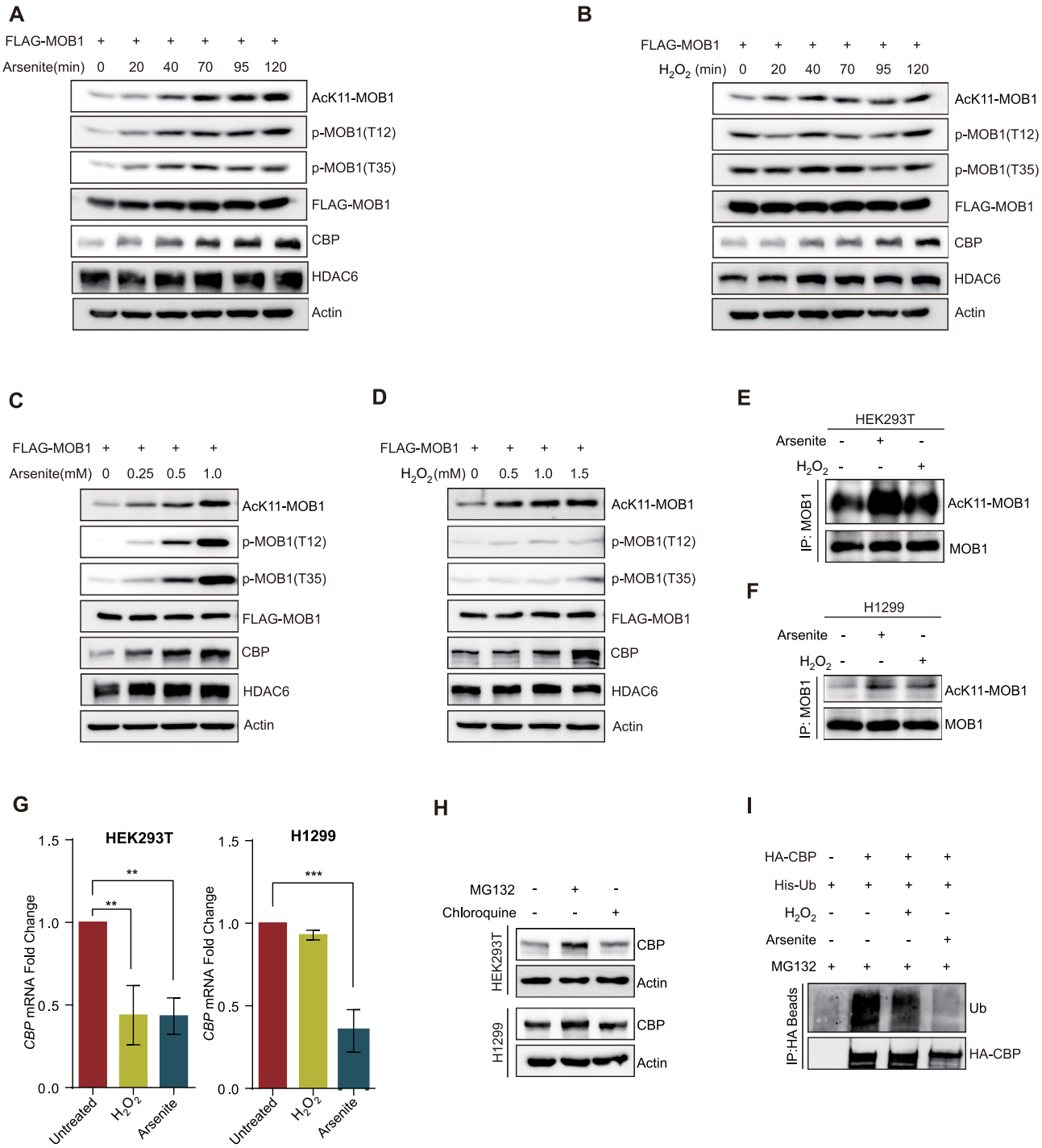

Figure 5. Oxidative stress-CBP axis regulates MOB1 acetylation. (**A** and **B**) HEK293T cells transiently expressing FLAG-MOB1 were treated with 1 mM sodium arsenite (A) or 1 mM H_2O_2 (B) for different time as indicated before harvesting. Cell lysates were performed SDS-PAGE and followed by immunoblotting with indicated antibodies. (**C** and **D**) FLAG-MOB1 plasmids were transiently transfected into HEK293T cells, which were treated with different concentrations of sodium arsenite (C) or H_2O_2 (D) for 1 h before harvesting. Cell lysates were subjected to SDS-PAGE and followed by immunoblotting with indicated antibodies. (**E** and **F**) Wild-type HEK293T cells (E) or H1299 cells (F) were treated with 1 mM sodium arsenite or 1 mM H_2O_2 for 1 h before harvesting. Cell lysates were subjected to immunoprecipitation with MOB1 Ab and western blot analysis, and then detected by AcK11-MOB1 Ab and MOB1 Ab. (**G**) Endogenous *CBP* expression levels in HEK293T (left part) and H1299 cells (right part) were detected by qPCR after treatment with 1 mM H_2O_2 or 1 mM sodium arsenite for 1 h. Statistical analyses were performed by GraphPad Prism 6, and error bars represented means ± SD. According to one-way ANOVA, ** is for $P < 0.01$ and *** is for $P < 0.001$. Images and statistical results were based on three independent experiments. (**H**) HEK293T (upper part) and H1299 cells (bottom part) were cultured in medium added 25 μM MG132 or 50 μM Chloroquine for 12 h before harvesting. Cell lysates were separated by SDS-PAGE and then immunoblotted with antibodies to CBP and Actin. (**I**) HA-tagged vector or HA-CBP together with His-Ubiquitin plasmids were cotransfected into HEK293T cells, which were treated with 25 μM MG132 for 12 h combined with 1 mM sodium arsenite or H_2O_2 for 1 h before harvesting. Cell lysates were subjected to immunoprecipitation with HA-Affinity Beads (anti-HA) and then immunoblotted with antibodies to Ubiquitin and HA.

MG132 treatment, suggesting that CBP is regulated by the ubiquitination–proteasome-mediated degradation pathway (Figure 5H). Furthermore, in H_2O_2 or sodium arsenite–treated HEK293T cells, the ubiquitination of CBP was decreased, especially when treated with sodium arsenite (Figure 5I). Therefore, oxidative stress promotes MOB1 acetylation by inhibiting CBP ubiquitination and enhancing the stability of CBP.

As shown in Figure 5A–D, MOB1 phosphorylation at T12 and T35 was also enhanced when treated with the two oxidative stress inducers, particularly in the presence of sodium arsenite (Figure 5A,C). However, the aforementioned findings demonstrated that phosphorylation of MOB1 affects its acetylation, which can also respond to oxidative stress. Thus, we wanted to determine whether MOB1 acetylation is modulated by MOB1 phosphorylation or by oxidative stress–regulated CBP. HEK293T cells were transfected with FLAG-MOB1-T12/35A mutant separately and treated with or without sodium arsenite (Supplementary Figure S5B) or H_2O_2 (Supplementary Figure S5C). The results showed that MOB1 acetylation can still be increased by oxidative stress even without MOB1 phosphorylation, suggesting that MOB1 phosphorylation at T12 and T35 is not required for its acetylation in response to oxidative stress. To determine whether the upstream kinases MST1/2 are involved in the regulation of MOB1 acetylation under oxidative stress, we knocked down endogenous MST1/2 using siRNAs (Supplementary Figure S5D) or treated with the inhibitor XMU-MP-1 in advance (Supplementary Figure S5E, S5F), and then added sodium arsenite or H_2O_2. These experiments indicated that MOB1 acetylation can be increased even when MST1/2 is depleted or inhibited (Supplementary Figure S5D–S5F), suggesting that MST1/2 and its kinase activity are also not required under these circumstances. These data indicated that oxidative stress-regulated MOB1 acetylation is mainly controlled by the oxidative stress-CBP axis and is independent of the upstream MST1/2 and MOB1 phosphorylation.

MOB1 acetylation mediates oxidative stress regulation of the Hippo pathway

The above findings indicated that acetylation stabilizes MOB1 (Figure 3). Therefore, we wanted to clarify whether oxidative stress-regulated MOB1 stability is mediated by the acetylation of MOB1. At first, we detected the protein level of MOB1 when treated with H_2O_2 (Supplementary Figure S6A) or NAC (Supplementary Figure S6B), which exhibited a significant enhancement or decline respectively (Supplementary Figure S6A, S6B). Next, H1299 (Figure 6A) and HEK293T cells (Supplementary Figure S6C) were cultured in medium with or without NAC, and the cells were treated with CHX for the indicated hours before harvesting. The results showed that the half–life of endogenous MOB1 decreased to approximately 7–10 h in the NAC–treated group compared to the control group, as shown in the quantitative studies (Figure 6A, Supplementary Figure S6C, and Figure 6B, Supplementary Figure S6D for quantification). However, the FLAG-MOB1-K11R mutant exhibited a half-life of approximately 7–10 h with or without NAC treatment, since it could not be acetylated (Figure 6C, Supplementary Figure S6E, and Figure 6D, Supplementary Figure S6F for quantification). These data indicated that both lack of oxidative stress and without MOB1 acetylation can destabilize MOB1. To answer whether oxidative stress affects MOB1 ubiquitination, we transfected FLAG-MOB1 and HA-ubiquitin in H1299 (Figure 6E) or HEK293T (Supplementary Figure S6G) cells, then treated cells with H_2O_2, sodium arsenite or NAC, and finally detected the ubiquitination level. The results showed that oxidative stress can reduce the ubiquitination of MOB1 and NAC, the inhibitor of stress, can reverse this effect (Figure 6E and Supplementary Figure S6G). These findings indicated that stress-induced MOB1 acetylation and stability are regulated by the ubiquitination of MOB1.

Furthermore, to explore whether MOB1–K11 acetylation causes a difference in activation of the Hippo pathway in response to oxidative stress, we transfected FLAG-MOB1-WT and K11R mutant in H1299 KO cells. Cells were treated with different concentrations of sodium arsenite for 1 h, and lysates were detected by western blot analysis. Compared with the MOB1-K11R group, phosphorylation of MOB1 at T35, LATS1 at T1079, YAP at S127 and S397 was enhanced more dramatically in the MOB1-WT group responding to arsenite treatment (Figure 6F). Additionally, the level of phosphorylation of YAP at S127 (p-YAP (S127) / YAP), which is closely related to its nuclear import, showed a significant difference (Figure 6G). Furthermore, we also tested the response of YAP acetylation to oxidative stress, which exhibited no significant change after 1 mM sodium arsenite or H_2O_2 treatment for 1 h (Supplementary Figure S6H, S6I). These findings indicated that arsenite or H_2O_2 have no significant effect on YAP acetylation. Taken together, CBP-MOB1 acetylation is one of the important cascades through which oxidative stress regulates activation of the Hippo pathway.

MOB1 acetylation regulates lung cancer progression

To examine the role of MOB1 acetylation in lung cancer progression, we established H1299 cells stably expressing FLAG-MOB1-WT or K11R mutant (Supplementary Figure S7A). Interestingly, we found that MOB1 inhibited, while the MOB1-K11R mutant promoted, lung cancer cell proliferation compared to the vector-transfected cells (Supplementary Figure S7B). Similarly, MOB1 inhibited, but MOB1-K11R accelerated, the formation and growth of cell colonies (Supplementary Figure S7C). Furthermore, we found that MOB1 inhibited lung cancer cell migration and invasion, whereas the MOB1-K11R mutant promoted lung cancer cell migration and invasion (Supplementary Figure S7D, S7E). The same trend that MOB1 suppressed and MOB1-K11R mutant promoted tumor growth was also observed in a tumor xenograft model (Figure 7A,B). The tumors in the acetylation-deficient MOB1-K11R mutant group were much larger and heavier compared to the control groups (Figure 7C,D). In summary, MOB1-K11 acetylation plays an important role in the suppression of lung cancer cell proliferation, migration, invasion *in vitro* and tumor growth *in vivo*.

To examine whether MOB1 acetylation is linked to the progression of lung cancer clinically, we evaluated the level

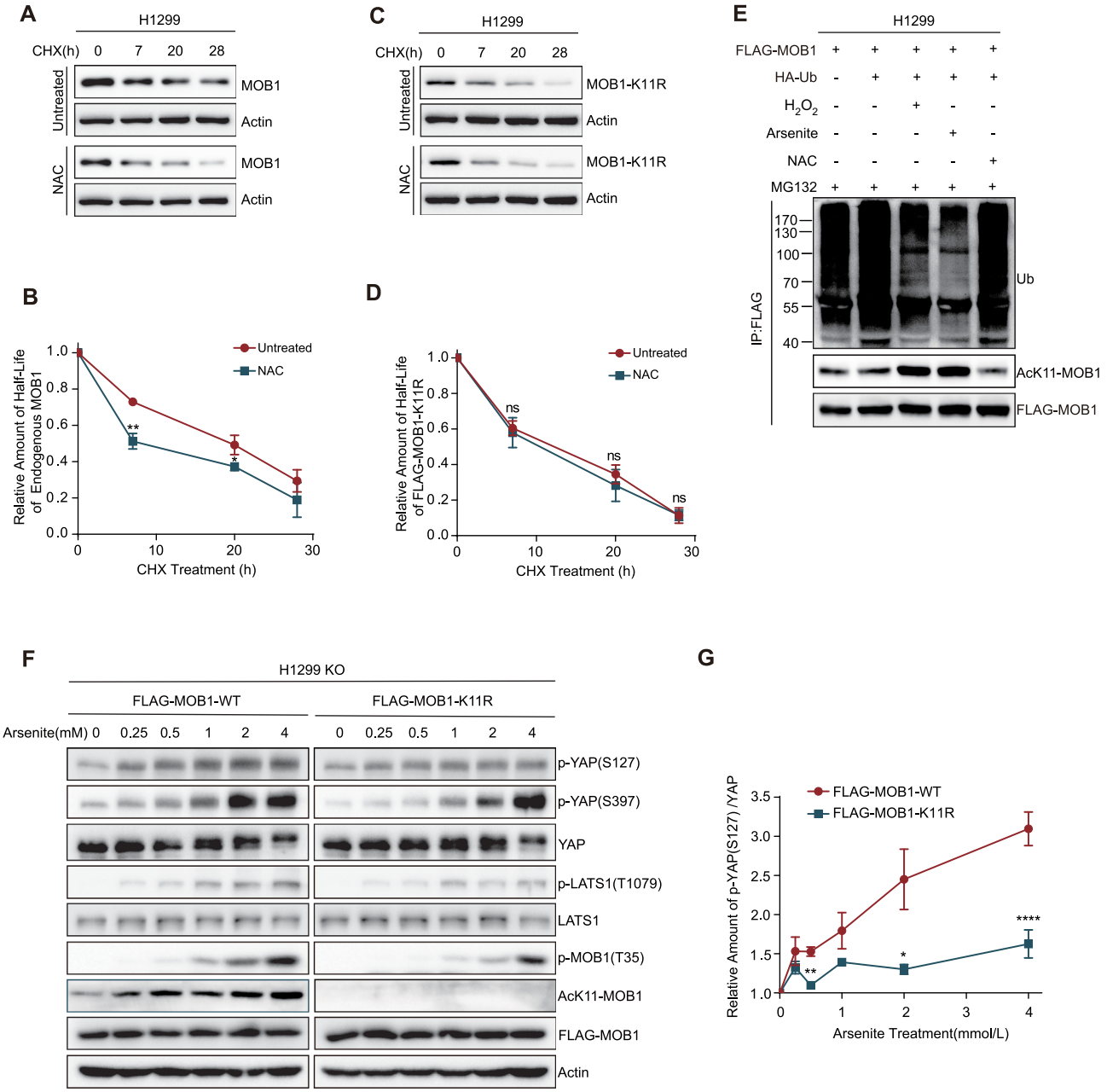

Figure 6. MOB1 acetylation mediates oxidative stress regulation of the Hippo pathway. (**A** and **B**) H1299 cells were incubated in the culture medium with or without 1 mM NAC, and treated with 100 mg/mL CHX for indicated hours before harvesting. Cells were lysed and endogenous MOB1 were detected by western blot analysis with MOB1 Ab (A). The curves were plotted based on the gray value of the bands of endogenous MOB1 in (A) by software Image J and GraphPad Prism 6. Error bars represented means ± SD. According to two-tailed Student's *t*-test,* is for $P < 0.05$ and ** is for $P < 0.01$. Images and statistical results were based on three independent experiments (B). (**C** and **D**) H1299 cells were transfected with FLAG-MOB1-K11R mutant plasmids, cultured in medium with or without 1 mM NAC and treated with 100 mg/ml CHX for indicated hours before harvesting. Cell lysates were subjected to western blot analysis with FLAG Ab and Actin Ab (C). The curves were plotted based on the grey value of the bands of FLAG-MOB1-K11R mutant in (C) by software ImageJ and GraphPad Prism 6. Error bars represented means ± SD. According to two-tailed Student's *t*-test, 'ns' is for no significance, $P > 0.05$. Images and statistical results were based on three independent experiments (D). (**E**) FLAG-MOB1 and HA-Ubiquitin were coexpressed in H1299 cells and treated with 25 μM MG132 for 12 h combined with 1 mM sodium arsenite for 1 h, 1 mM H_2O_2 for 1 h or 1 mM NAC for 12–24 h before harvesting. Cell lysates were subjected to immunoprecipitation with M2-Beads (anti-FLAG), and then immunoblotted with the antibodies to Ubiquitin, FLAG and AcK11-MOB1. (**F** and **G**) Two groups of H1299 KO cells (each group consisted of six dishes) were transfected with FLAG-MOB1 (WT or K11R mutant) respectively, following by using different concentration of sodium arsenite to treat cells for 1 h before harvesting. Cells were lysed, implemented western blot analysis and analyzed by antibodies as indicated in the figure (F). The gray value of the bands of p-YAP (S127) and YAP was determined by software ImageJ. Relative amount of p-YAP (S127) / YAP was analyzed and plotted by GraphPad Prism 6. Error bars represented means ± SEM. According to two-tailed Student's *t*-test,* is for $P < 0.05$, ** is for $P < 0.01$ and **** is for $P < 0.0001$. Images and statistical results were based on three independent experiments (G).

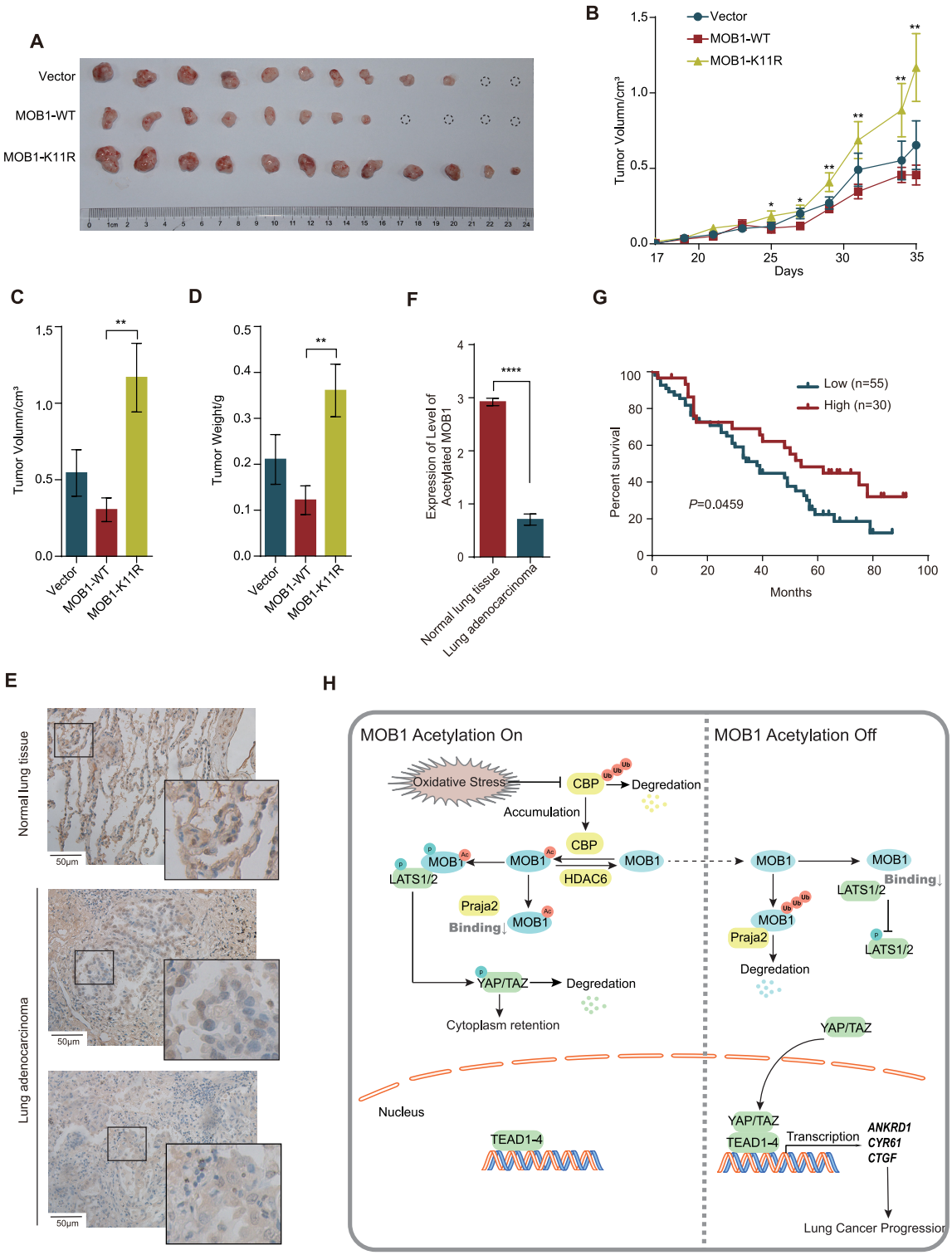

Figure 7. MOB1 acetylation regulates lung cancer progression. (**A–D**) H1299 cells stably expressing Vector, FLAG-MOB1 (WT or K11R mutant) were injected into axillas of nude mice and the xenograft tumors were dissevered at the day 35. All tumor masses were illustrated in (A). The size of tumors were evaluated and recorded every 2 days, from day 17 when tumors formed (B). The ultimate volume (C) and weight (D) were measured simultaneously after surgery at day 35, which were shown as mean ± SEM in histogram. According to one-way ANOVA, *is for $P < 0.05$ and ** is for $P < 0.01$. (**E** and **F**) Immunohistochemical stain was performed using AcK11-MOB1 Ab and representative images of normal lung tissues (upper part) and lung adenocarcinoma tissues, including strongly stained group (middle part) and weakly stained group (bottom part), were displayed in figure (E). The lower right corner of each image was magnified locally; scale bar: 50 μm, $n = 85$ (E). Levels of MOB1-K11 acetylation in normal lung tissues and lung adenocarcinoma tissues were statistically analyzed and exhibited as mean ± SEM in column diagrams. According to Mann–Whitney test, **** is for $P < 0.0001$ (F). (**G**) Kaplan–Meier analysis was accomplished in low MOB1-K11 acetylation group ($n = 55$) and high acetylation group ($n = 30$). According to Log-rank (Mantel–Cox) test, P value is 0.0459 for *, $n = 85$. (**H**) A working model of MOB1 acetylation in the Hippo signaling pathway.

of MOB1-K11 acetylation in a cohort of 85 lung adenocarcinoma patients by immunohistochemical analysis. The results showed that MOB1-K11 acetylation was markedly decreased in lung adenocarcinoma patients, whereas MOB1-K11 acetylation was much stronger in normal lung tissues (Figure 7E, and F for quantification). Notably, the level of MOB1-K11 acetylation was correlated with the prognosis of patients, and hyperacetylation led to a better overall survival in NSCLC patients (Figure 7G). Taken together, MOB1-K11 acetylation suppresses lung cancer progression.

DISCUSSION

Components of the Hippo signaling pathway are modulated by various PTMs, including phosphorylation, ubiquitination, methylation and acetylation, which affect activation and subcellular localization of the key transcriptional cofactors, YAP/TAZ. For instance, deacetylation of MST1 by HDAC6 results in a decrease in protein stability and progression of breast cancer (27). YAP itself is acetylated by CBP/p300 at lysine 494 and 497, and deacetylated by SIRT1, affecting its nuclear translocation and interaction with TEAD, and changing its transcriptional activity and tumorigenesis (29). In this study, we demonstrated a novel modification of the Hippo signaling scaffold molecule MOB1 by identifying its acetylation by CBP and deacetylation by HDAC6. Importantly, acetylation confers MOB1 with enhanced stability and a high ability to initiate LATS1 kinase activity, ultimately leading to strong YAP/TAZ phosphorylation. Moreover, acetylation of MOB1 is modulated by cellular oxidative stress upstream, a physiological link that emphasizes the importance of this modification. Therefore, we proposed a new mechanism involving oxidative stress–regulated MOB1 acetylation, which controls the activation of Hippo, suppression of lung adenocarcinoma cell growth and patient prognosis (Figure 7H).

MOB1, as a coactivator of LATS1/2 kinase, is considered to be a potential tumor suppressor. It has been reported that the mRNA level of human MOB1 is significantly decreased in NSCLC patients and associated with tumor invasion (60). In addition, MOB1 inhibits proliferation and migration of colorectal cancer cells, decreases the incidence of lymph node or distant metastasis and promotes a better prognosis in patients with colorectal cancer (61). However, deletion of MOB1 may cause bronchiolar cells and bronchioalveolar stem cells to separate from the basement membrane in adult mouse lungs and suppress tumor initiation (62). An analysis of 205 lung cancer patients showed that high MOB1 expression was associated with poor disease-free survival and intratumoral vascular invasion (63). Therefore, studies on MOB1 function should not be limited to its expression level, and different PTMs of MOB1 need to be considered. In this study, we revealed that acetylated MOB1 inhibits, while non-acetylated MOB1 promotes formation and growth of lung adenocarcinoma *in vivo* and *in vitro*. Mechanically, acetylation stabilizes MOB1 by weakening its interaction with the E3 ligase Praja2, and reducing the proteasome-mediated degradation of MOB1. In addition, MOB1-K11 acetylation increases its phosphorylation and enhances MOB1 binding capacity with LATS1, leading to enhanced LATS1 phosphorylation at T1079 and activation of the Hippo pathway. As a result, acetylation of MOB1 leads to hyper-phosphorylation of YAP/TAZ and suppresses Hippo target genes expression, including *ANKRD1*, *CTGF* and *CYR61*, which control cell proliferation, differentiation, apoptosis and angiogenesis.

To determine the physiological or pathological conditions that trigger the acetylation of MOB1, we investigated a variety of upstream stimuli of the Hippo pathway. Among them, oxidative stress affects core components of the Hippo signaling pathway, MST1/2 (32–34,64), LATS1/2 (65) and YAP (35–37,66). In this study, we demonstrated that oxidative stress induces MOB1 acetylation, which controls LATS1 activation. Increasing amounts of reactive oxygen species (ROS) stabilize the acetyltransferase CBP, and then promote acetylation and stabilization of MOB1. Thus, the MOB1-LATS1 interaction is enhanced, and LATS1 activation is promoted. Consequently, YAP/TAZ is hyperphosphorylated by LATS1, hinders YAP/TAZ nuclear translocation and may suppress the transcription of anti–apoptosis and antioxidation target genes. Therefore, oxidative stress can regulate the Hippo signaling pathway through an alternative mechanism involving the oxidative stress-MOB1-LATS1 signaling cascade.

It has been reported that the incidence and mortality of lung cancer remains high throughout the world. Among all the cases, 80% are NSCLC, which has the characteristics of short survival time, high recurrence rate and high drug resistance (20). Therefore, the development of effective therapeutic drugs and early detection has become an urgent problem. Some anticancer therapies have been proved to cause tumor cell death by generating ROS. For instance, cisplatin and γ-irradiation can promote oxidative stress, leading to a cluster of Fas receptors and cell death (67). In $CD4^+$ T cell–based adoptive immunotherapy, T-cell–derived TNF-α can cooperate with chemotherapy drugs to reinforce oxidative stress and promote tumor cell death via NADPH oxidase (68). Based on this study, we assumed that activation of the Hippo pathway may have broad applications in the rational use of reactive oxygen species to cure cancers. Applying oxidative stress–related drugs may activate Hippo/YAP pathway in patients through MOB1 acetylation. Moreover, deacetylation of MOB1 may attenuate the therapeutic effect; therefore, appropriately increasing MOB1 acetylation may be of choice in lung cancer therapy. Alternatively, evaluation of the acetylation status of MOB1–K11 may be of diagnostic value, which reflects the tumor progression and prognosis.

In summary, we demonstrated that acetylation of MOB1 at K11 by CBP stabilizes MOB1 and promotes LATS1 activation and YAP/TAZ phosphorylation in an oxidative stress–regulated manner. Acetylated MOB1 suppresses lung cancer cell growth and invasion, and increased acetylation of MOB1 leads to better patient survival in lung adenocarcinomas.

DATA AVAILABILITY

We comply with the 'Minimal Information for Publication of Quantitative Real-Time PCR Experiments' (MIQE) guidelines. And other details, including the sequences of siRNA and primers that used in the quantitative Real-Time

PCR, are supplied in Materials and Methods section of this manuscript.

SUPPLEMENTARY DATA

Supplementary Data are available at NAR Online.

ACKNOWLEDGEMENTS

We thank Dr Jun Zhou for providing HA–HDAC6 plasmid kindly and Jing Zhang for help in the immunohistochemical experiments. We also thank Yuhan Jiang, Cheng Liu, Yixiao Li and Xiaolin Tian for the helpful discussions.

FUNDING

Ministry of Science and Technology of China [2021YFC2501000]; National Natural Science Foundation of China [81730071, 81972616, 81230051, 81972609, 81773199]; Beijing Natural Science Foundation [7171005, 7202084]; Shanghai Science and Technology Commission [20JC1410100]; Peking University grant [PKU2021LCXQ023 to H.Z. and J.Z.]. Funding for open access charge: National Natural Science Foundation of China [81730071].
Conflict of interest statement. None declared.

REFERENCES

1. Pan,D.J. (2010) The hippo signaling pathway in development and cancer. *Dev. Cell*, **19**, 491–505.
2. Yu,F.X., Zhao,B. and Guan,K.L. (2015) Hippo pathway in organ size control, tissue homeostasis, and cancer. *Cell*, **163**, 811–828.
3. Meng,Z.P., Moroishi,T. and Guan,K.L. (2016) Mechanisms of Hippo pathway regulation. *Genes Dev*., **30**, 1–17.
4. Zhao,B., Li,L., Lei,Q.Y. and Guan,K.L. (2010) The Hippo-YAP pathway in organ size control and tumorigenesis: an updated version. *Genes Dev*., **24**, 862–874.
5. Cai,J., Zhang,N.L., Zheng,Y.G., de Wilde,R.F., Maitra,A. and Pan,D.J. (2010) The Hippo signaling pathway restricts the oncogenic potential of an intestinal regeneration program. *Genes Dev*., **24**, 2383–2388.
6. Hou,M.C., Wiley,D.J., Verde,F. and McCollum,D. (2003) Mob2p interacts with the protein kinase Orb6p to promote coordination of cell polarity with cell cycle progression. *J. Cell Sci.*, **116**, 125–135.
7. Luca,F.C., Mody,M., Kurischko,C., Roof,D.M., Giddings,T.H. and Winey,M. (2001) Saccharomyces cerevisiae Mob1p is required for cytokinesis and mitotic exit. *Mol. Cell. Biol.*, **21**, 6972–6983.
8. Lai,Z.C., Wei,X., Shimizu,T., Ramos,E., Rohrbaugh,M., Nikolaidis,N., Ho,L.L. and Li,Y. (2005) Control of cell proliferation and apoptosis by mob as tumor suppressor, mats. *Cell*, **120**, 675–685.
9. Wei,X., Shimizu,T. and Lai,Z.C. (2007) Mob as tumor suppressor is activated by Hippo kinase for growth inhibition in Drosophila. *EMBO J*., **26**, 1772–1781.
10. Ni,L., Zheng,Y., Hara,M., Pan,D. and Luo,X. (2015) Structural basis for Mob1-dependent activation of the core Mst–Lats kinase cascade in hippo signaling. *Genes Dev*., **29**, 1416–1431.
11. Kim,S.Y., Tachioka,Y., Mori,T. and Hakoshima,T. (2016) Structural basis for autoinhibition and its relief of MOB1 in the Hippo pathway. *Sci. Rep.*, **6**, 28488.
12. Praskova,M., Xia,F. and Avruch,J. (2008) MOBKL1A/MOBKL1B phosphorylation by MST1 and MST2 inhibits cell proliferation. *Curr. Biol.*, **18**, 311–321.
13. Hergovich,A., Schmitz,D. and Hemmings,B.A. (2006) The human tumour suppressor LATS1 is activated by human MOB1 at the membrane. *Biochem. Biophys. Res. Commun.*, **345**, 50–58.
14. Yin,F., Yu,J., Zheng,Y., Chen,Q., Zhang,N. and Pan,D. (2013) Spatial organization of Hippo signaling at the plasma membrane mediated by the tumor suppressor Merlin/NF2. *Cell*, **154**, 1342–1355.
15. Chan,E.H., Nousiainen,M., Chalamalasetty,R.B., Schafer,A., Nigg,E.A. and Sillje,H.H.W. (2005) The Ste20-like kinase Mst2 activates the human large tumor suppressor kinase Lats1. *Oncogene*, **24**, 2076–2086.
16. Zhao,B., Wei,X., Li,W., Udan,R.S., Yang,Q., Kim,J., Xie,J., Ikenoue,T., Yu,J., Li,L. *et al.* (2007) Inactivation of YAP oncoprotein by the Hippo pathway is involved in cell contact inhibition and tissue growth control. *Genes Dev*., **21**, 2747–2761.
17. Lei,Q.Y., Zhang,H., Zhao,B., Zha,Z.Y., Bai,F., Pei,X.H., Zhao,S., Xiong,Y. and Guan,K.L. (2008) TAZ promotes cell proliferation and epithelial-mesenchymal transition and is inhibited by the hippo pathway. *Mol. Cell. Biol.*, **28**, 2426–2436.
18. Hao,Y., Chun,A., Cheung,K., Rashidi,B. and Yang,X. (2008) Tumor suppressor LATS1 is a negative regulator of oncogene YAP. *J. Biol. Chem.*, **283**, 5496–5509.
19. Sanchez-Vega,F., Mina,M., Armenia,J., Chatila,W.K., Luna,A., La,K.C., Dimitriadoy,S., Liu,D.L., Kantheti,H.S., Saghafinia,S. *et al.* (2018) Oncogenic signaling pathways in the cancer genome atlas. *Cell*, **173**, 321–337.
20. Cai,J., Fang,L., Huang,Y., Li,R., Yuan,J., Yang,Y., Zhu,X., Chen,B., Wu,J. and Li,M. (2013) miR-205 targets PTEN and PHLPP2 to augment AKT signaling and drive malignant phenotypes in non-small cell lung cancer. *Cancer Res*., **73**, 5402–5415.
21. Sung,H., Ferlay,J., Siegel,R.L., Laversanne,M., Soerjomataram,I., Jemal,A. and Bray,F. (2021) Global cancer statistics 2020: GLOBOCAN estimates of incidence and mortality worldwide for 36 cancers in 185 countries. *Ca-Cancer J. Clin.*, **71**, 209–249.
22. Xu,C.M., Liu,W.W., Liu,C.J., Wen,C., Lu,H.F. and Wan,F.S. (2013) Mst1 overexpression inhibited the growth of human non-small cell lung cancer in vitro and in vivo. *Cancer Gene Ther*., **20**, 453–460.
23. Xia,H., Qi,H., Li,Y., Pei,J., Barton,J, Blackstad,M. and Tao,W. (2002) LATS1 tumor suppressor regulates G2/M transition and apoptosis. *Oncogene*, **21**, 1233–1241.
24. Hirabayashi,S., Nakagawa,K., Sumita,K., Hidaka,S., Kawai,T., Ikeda,M., Kawata,A., Ohno,K. and Hata,Y. (2008) Threonine 74 of MOB1 is a putative key phosphorylation site by MST2 to form the scaffold to activate nuclear Dbf2-related kinase 1. *Oncogene*, **27**, 4281–4292.
25. Song,Z., Han,X., Zou,H., Zhang,B., Ding,Y., Xu,X., Zeng,J., Liu,J. and Gong,A. (2018) PTEN-GSK3beta-MOB1 axis controls neurite outgrowth in vitro and in vivo. *Cell. Mol. Life Sci.*, **75**, 4445–4464.
26. Lignitto,L., Arcella,A., Sepe,M., Rinaldi,L., Delle Donne,R., Gallo,A., Stefan,E., Bachmann,V.A., Oliva,M.A., Tiziana Storlazzi,C. *et al.* (2013) Proteolysis of MOB1 by the ubiquitin ligase praja2 attenuates Hippo signalling and supports glioblastoma growth. *Nat. Commun.*, **4**, 1822.
27. Li,L., Fang,R., Liu,B., Shi,H., Wang,Y., Zhang,W., Zhang,X. and Ye,L. (2016) Deacetylation of tumor-suppressor MST1 in Hippo pathway induces its degradation through HBXIP-elevated HDAC6 in promotion of breast cancer growth. *Oncogene*, **35**, 4048–4057.
28. Yang,S., Xu,W., Liu,C., Jin,J., Li,X., Jiang,Y., Zhang,L., Meng,X., Zhan,J. and Zhang,H. (2022) LATS1 K751 acetylation blocks activation of Hippo signalling and switches LATS1 from a tumor suppressor to an oncoprotein. *Sci. China Life Sci.*, **65**, 129–141.
29. Hata,S., Hirayama,J., Kajiho,H., Nakagawa,K., Hata,Y., Katada,T., Furutani-Seiki,M. and Nishina,H. (2012) A novel acetylation cycle of transcription Co-activator Yes-associated protein that is downstream of hippo pathway is triggered in response to S(N)2 alkylating agents. *J. Biol. Chem.*, **287**, 22089–22098.
30. Schieber,M. and Chandel,N.S. (2014) ROS function in redox signaling and oxidative stress. *Curr. Biol.*, **24**, R453–R462.
31. Hayes,J.D., Dinkova-Kostova,A.T. and Tew,K.D. (2020) Oxidative stress in cancer. *Cancer Cell*, **38**, 167–197.
32. Lehtinen,M.K., Yuan,Z., Boag,P.R., Yang,Y., Villen,J., Becker,E.B., DiBacco,S., de la Iglesia,N., Gygi,S., Blackwell,T.K. *et al.* (2006) A conserved MST-FOXO signaling pathway mediates oxidative-stress responses and extends life span. *Cell*, **125**, 987–1001.
33. Xiao,L., Chen,D., Hu,P., Wu,J., Liu,W., Zhao,Y., Cao,M., Fang,Y., Bi,W., Zheng,Z. *et al.* (2011) The c-Abl-MST1 signaling pathway mediates oxidative stress-induced neuronal cell death. *J. Neurosci.*, **31**, 9611–9619.
34. Morinaka,A., Funato,Y., Uesugi,K. and Miki,H. (2011) Oligomeric peroxiredoxin-I is an essential intermediate for p53 to activate MST1 kinase and apoptosis. *Oncogene*, **30**, 4208–4218.

35. Chen,T., Zhao,L., Chen,S., Zheng,B., Chen,H., Zeng,T., Sun,H., Zhong,S., Wu,W., Lin,X. *et al.* (2020) The curcumin analogue WZ35 affects glycolysis inhibition of gastric cancer cells through ROS-YAP-JNK pathway. *Food Chem. Toxicol.*, **137**, 111131.
36. Wang,L., Wang,C., Tao,Z., Zhao,L., Zhu,Z., Wu,W., He,Y., Chen,H., Zheng,B., Huang,X. *et al.* (2019) Curcumin derivative WZ35 inhibits tumor cell growth via ROS-YAP-JNK signaling pathway in breast cancer. *J. Exp. Clin. Cancer Res.*, **38**, 460.
37. Cucci,M.A., Compagnone,A., Daga,M., Grattarola,M., Ullio,C., Roetto,A., Palmieri,A., Rosa,A.C., Argenziano,M., Cavalli,R. *et al.* (2019) Post-translational inhibition of YAP oncogene expression by 4-hydroxynonenal in bladder cancer cells. *Free Radical Biol. Med.*, **141**, 205–219.
38. Cao,X., Li,C., Xiao,S., Tang,Y., Huang,J., Zhao,S., Li,X., Li,J., Zhang,R. and Yu,W. (2017) Acetylation promotes TyrRS nuclear translocation to prevent oxidative damage. *Proc. Natl. Acad. Sci. U.S.A.*, **114**, 687–692.
39. Li,C. and Yu,W. (2017) Reversible lysine acetylation regulates nuclear translocation of TyrRS to counteract genotoxic oxidative stress. *Mol. Cell. Oncol.*, **4**, e1293597.
40. Kwon,J., Lee,S., Kim,Y.N. and Lee,I.H. (2019) Deacetylation of CHK2 by SIRT1 protects cells from oxidative stress-dependent DNA damage response. *Exp. Mol. Med.*, **51**, 36.
41. Wang,Y.P., Zhou,L.S., Zhao,Y.Z., Wang,S.W., Chen,L.L., Liu,L.X., Ling,Z.Q., Hu,F.J., Sun,Y.P., Zhang,J.Y. *et al.* (2014) Regulation of G6PD acetylation by SIRT2 and KAT9 modulates NADPH homeostasis and cell survival during oxidative stress. *EMBO J.*, **33**, 1304–1320.
42. Seo,J.H., Park,J.H., Lee,E.J., Vo,T.T., Choi,H., Kim,J.Y., Jang,J.K., Wee,H.J., Lee,H.S., Jang,S.H. *et al.* (2016) ARD1-mediated Hsp70 acetylation balances stress-induced protein refolding and degradation. *Nat. Commun.*, **7**, 12882.
43. Saito,M., Hess,D., Eglinger,J., Fritsch,A.W., Kreysing,M., Weinert,B.T., Choudhary,C. and Matthias,P. (2018) Acetylation of intrinsically disordered regions regulates phase separation. *Nat. Chem. Biol.*, **15**, 51–61.
44. Sarikhani,M., Mishra,S., Desingu,P.A., Kotyada,C., Wolfgeher,D., Gupta,M.P., Singh,M. and Sundaresan,N.R. (2018) SIRT2 regulates oxidative stress-induced cell death through deacetylation of c-Jun NH2-terminal kinase. *Cell Death Differ.*, **25**, 1638–1656.
45. Song,J., Wang,T., Chi,X., Wei,X., Xu,S., Yu,M., He,H., Ma,J., Li,X., Du,J. *et al.* (2019) Kindlin-2 inhibits the Hippo signaling pathway by promoting degradation of MOB1. *Cell Rep.*, **29**, 3664–3677.
46. Narita,T., Weinert,B.T. and Choudhary,C. (2019) Functions and mechanisms of non-histone protein acetylation. *Nat. Rev. Mol. Cell Biol.*, **20**, 156–174.
47. Ali,I., Conrad,R.J., Verdin,E. and Ott,M. (2018) Lysine acetylation goes global: from epigenetics to metabolism and therapeutics. *Chem. Rev.*, **118**, 1216–1252.
48. Paz,J.C., Park,S.H., Phillips,N., Matsumura,S., Tsai,W.W., Kasper,L., Brindle,P.K., Zhang,G.T., Zhou,M.M., Wright,P.E. *et al.* (2014) Combinatorial regulation of a signal-dependent activator by phosphorylation and acetylation. *Proc. Natl. Acad. Sci. U.S.A.*, **111**, 17116–17121.
49. Wang,D.L., Kon,N., Lasso,G., Jiang,L., Leng,W.C., Zhu,W.G., Qin,J., Honig,B. and Gu,W. (2016) Acetylation-regulated interaction between p53 and SET reveals a widespread regulatory mode. *Nature*, **538**, 118–122.
50. Cao,X.Y., Li,C.Q., Xiao,S.Y., Tang,Y.L., Huang,J., Zhao,S., Li,X.Y., Li,J.X., Zhang,R.L. and Yu,W. (2017) Acetylation promotes TyrRS nuclear translocation to prevent oxidative damage. *Proc. Natl. Acad. Sci. U.S.A.*, **114**, 687–692.
51. Santos-Rosa,H., Valls,E., Kouzarides,T. and Martinez-Balbas,M. (2003) Mechanisms of P/CAF auto-acetylation. *Nucleic Acids Res.*, **31**, 4285–4292.
52. Thompson,P.R., Wang,D.X., Wang,L., Fulco,M., Pediconi,N., Zhang,D.Z., An,W.J., Ge,Q.Y., Roeder,R.G., Wong,J.M. *et al.* (2004) Regulation of the p300 HAT domain via a novel activation loop. *Nat. Struct. Mol. Biol.*, **11**, 308–315.
53. Sun,B.F., Guo,S.L., Tang,Q.Y., Li,C., Zeng,R., Xiong,Z.Q., Zhong,C. and Ding,J.P. (2011) Regulation of the histone acetyltransferase activity of hMOF via autoacetylation of Lys274. *Cell Res.*, **21**, 1262–1266.
54. Barlev,N.A., Liu,L., Chehab,N.H., Mansfield,K., Harris,K.G., Halazonetis,T.D. and Berger,S.L. (2001) Acetylation of p53 activates transcription through recruitment of coactivators/histone acetyltransferases. *Mol. Cell*, **8**, 1243–1254.
55. Wan,J., Zhan,J., Li,S., Ma,J., Xu,W., Liu,C., Xue,X., Xie,Y., Fang,W., Chin,Y.E. *et al.* (2015) PCAF-primed EZH2 acetylation regulates its stability and promotes lung adenocarcinoma progression. *Nucleic Acids Res.*, **43**, 3591–3604.
56. Chen,Y., Huang,Q., Liu,W., Zhu,Q., Cui,C.P., Xu,L., Guo,X., Wang,P., Liu,J., Dong,G. *et al.* (2018) Mutually exclusive acetylation and ubiquitylation of the splicing factor SRSF5 control tumor growth. *Nat. Commun.*, **9**, 2464.
57. Yu,F.X. and Guan,K.L. (2013) The Hippo pathway: regulators and regulations. *Genes Dev.*, **27**, 355–371.
58. Misra,J.R. and Irvine,K.D. (2018) The Hippo signaling network and its biological functions. *Annu. Rev. Genet.*, **52**, 65–87.
59. Wang,P., Geng,J., Gao,J., Zhao,H., Li,J., Shi,Y., Yang,B., Xiao,C., Linghu,Y., Sun,X. *et al.* (2019) Macrophage achieves self-protection against oxidative stress-induced ageing through the Mst-Nrf2 axis. *Nat. Commun.*, **10**, 755.
60. Sasaki,H., Kawano,O., Endo,K., Suzuki,E., Yukiue,H., Kobayashi,Y., Yano,M. and Fujii,Y. (2007) Human MOB1 expression in non-small-cell lung cancer. *Clin. Lung Cancer*, **8**, 273–276.
61. Liu,J., Shi,Z., Ma,Y., Fu,L. and Yi,M. (2020) MOB1 inhibits malignant progression of colorectal cancer by targeting PAK2. *OncoTargets Ther.*, **13**, 8803–8811.
62. Otsubo,K., Goto,H., Nishio,M., Kawamura,K., Yanagi,S., Nishie,W., Sasaki,T., Maehama,T., Nishina,H., Mimori,K. *et al.* (2017) MOB1-YAP1/TAZ-NKX2.1 axis controls bronchioalveolar cell differentiation, adhesion and tumour formation. *Oncogene*, **36**, 4201–4211.
63. Ando,N., Tanaka,K., Otsubo,K., Toyokawa,G., Ikematsu,Y., Ide,M., Yoneshima,Y., Iwama,E., Inoue,H., Ijichi,K. *et al.* (2020) Association of Mps one binder kinase activator 1 (MOB1) expression with poor disease-free survival in individuals with non-small cell lung cancer. *Thorac. Cancer*, **11**, 2830–2839.
64. Roh,K.H. and Choi,E.J. (2016) TRAF2 functions as an activator switch in the reactive oxygen species-induced stimulation of MST1. *Free Radical Biol. Med.*, **91**, 105–113.
65. Rajesh,K., Krishnamoorthy,J., Gupta,J., Kazimierczak,U., Papadakis,A.I., Deng,Z., Wang,S., Kuninaka,S. and Koromilas,A.E. (2016) The eIF2α serine 51 phosphorylation-ATF4 arm promotes HIPPO signaling and cell death under oxidative stress. *Oncotarget*, **7**, 51044–51058.
66. Wu,H., Xiao,Y., Zhang,S., Ji,S., Wei,L., Fan,F., Geng,J., Tian,J., Sun,X., Qin,F. *et al.* (2013) The Ets transcription factor GABP is a component of the hippo pathway essential for growth and antioxidant defense. *Cell Rep.*, **3**, 1663–1677.
67. Huang,H.L., Fang,L.W., Lu,S.P., Chou,C.K., Luh,T.Y. and Lai,M.Z. (2003) DNA-damaging reagents induce apoptosis through reactive oxygen species-dependent Fas aggregation. *Oncogene*, **22**, 8168–8177.
68. Habtetsion,T., Ding,Z.C., Pi,W., Li,T., Lu,C., Chen,T., Xi,C., Spartz,H., Liu,K., Hao,Z. *et al.* (2018) Alteration of tumor metabolism by CD4+ T cells leads to TNF-alpha-Dependent intensification of oxidative stress and tumor cell death. *Cell Metab.*, **28**, 228–242.